

SAND79-1245
Unlimited Release
UC-70

Gas Generation From Transuranic Waste Degradation: Data Summary and Interpretation

Martin A. Molecke

Prepared by Sandia Laboratories, Albuquerque, New Mexico 87185
and Livermore, California 94550 for the United States Department
of Energy under Contract DE-AC04-76DP00769

Printed December 1979



Sandia Laboratories

Issued by Sandia Laboratories, operated for the United States Department of Energy by Sandia Corporation.

NOTICE

This report was prepared as an account of work sponsored by the United States Government. Neither the United States nor the Department of Energy, nor any of their employees, nor any of their contractors, subcontractors, or their employees, makes any warranty, express or implied, or assumes any legal liability or responsibility for the accuracy, completeness or usefulness of any information, apparatus, product or process disclosed, or represents that its use would not infringe privately owned rights.

Printed in the United States of America

Available from
National Technical Information Service
U. S. Department of Commerce
5285 Port Royal Road
Springfield, VA 22161

Price: Printed Copy \$6.00; Microfiche \$3.00

SAND79-1245
Unlimited Release
Submitted July 1979
Printed December 1979

GAS GENERATION FROM
TRANSURANIC WASTE DEGRADATION:
DATA SUMMARY AND INTERPRETATION*

Martin A. Molecke
Sandia Laboratories
Nuclear Waste Experimental Programs
Division 4512
Albuquerque, New Mexico 87185

ABSTRACT

A comprehensive review of all applicable gas generation data resulting from the degradation of existing and potential forms of transuranic-contaminated wastes is presented. Extensive experimental studies have been performed under both realistic environmental conditions expected in the Waste Isolation Pilot Plant and overtest conditions. Degradation mechanisms investigated were radiolysis, thermal decomposition and dewatering, bacterial action, and chemical corrosion. Waste matrices studied include cellulose, plastics, rubbers, organic composite, concrete-TRU ash, asphalt, process sludges, and mild steel. Measured gas generation rates are presented in terms of gas moles/year/drum of waste and in G(gas) values for radiolysis. The effects of multiple variables on gas generation are also described.

*This work supported by the U. S. Department of Energy

TABLE OF CONTENTS

	<u>PAGE</u>
ABSTRACT	i
TABLE OF CONTENTS	ii
LIST OF TABLES	iii
LIST OF FIGURES	iii
ACKNOWLEDGEMENTS	iv
1.0 INTRODUCTION	1
1.1 WIPP Environmental Conditions	3
1.2 Waste Form Characteristics	6
2.0 RADIOLYTIC DEGRADATION DATA	9
2.1 Dose Rate and Time Effects	11
2.2 Pressure Effects	14
2.3 Temperature Effects	15
2.4 Composition of Radiolysis Gases	16
2.5 Field Test Data	16
2.6 Concrete Matrix TRU Wastes	17
2.6.1 Effect of Dewatering	22
2.6.2 Pressed Concrete Radiolysis	23
2.6.3 Total Gas Generation and Pressurization	25
2.7 Assorted Radiolysis Observations	27
3.0 THERMAL DEGRADATION DATA	30
3.1 Threshold Decomposition Temperatures	30
3.2 Thermal Decomposition, Gas Generation	30
3.3 Thermal Dewatering	33
4.0 BACTERIAL DEGRADATION DATA	36
4.1 Experimental	37
4.2 Gas Generation Results and Discussion	38
5.0 CHEMICAL CORROSION DATA	45
6.0 SUMMARY OF RESULTS	47
7.0 REFERENCES	56

LIST OF TABLES

<u>TABLE</u>		<u>PAGE</u>
1	Gas Generation from TRU Wastes	2
2	Assumed Characteristics of Standard Drum (210 liter) Content	8
3	Radiolytic Degradation Data Summary, TRU Waste Contaminated Matrices	10
4a	Radiolysis Data of High Alumina Concrete-TRU Ash Samples	19
4b	Radiolysis Data of Portland Type I Concrete-TRU Ash Samples	20
5	Pressed Concrete Pellet Results	26
6	Threshold Decomposition Temperatures of Organic Waste Matrices	31
7	Tentative Gas Generation Rates from Thermal Degradation	34
8	Approximate Gas Compositions from Thermal Degradation at 70°C	34
9	Preliminary Gas Generation Rates from Bacterial Degradation	39
10	Degradation of Cellulosics Under Optimum Anaerobic Conditions	39
11	Net Bacterial CO ₂ Gas Generation for Various Environments	43
12	Mild Steel Corrosion and Gas Consumption/Generation	46
13	Observed Ranges of Initial Gas Generation Rates	49
14	Comparative Gas Generation Rates	52
15	Theoretical Total Gas Generation/Drum	55

LIST OF FIGURES

1	WIPP TRU CH Level Temperature	4
2	Regional Thermal Analysis Model	5
3	Cellulosic G Values Vs Integrated Dosage	13
4	Effect of Water in Concrete on Radiolytic Gas Production	24
5	Concrete-TRU Ash Matrix, Long-Term Pressure Increase per Drum	28
6	Bacterial Degradation of Organic Composite Waste versus Temperature	41
7	Comparative Gas Generation Rates	53

ACKNOWLEDGEMENTS

The assistance of Stan Kosiewicz of the Los Alamos Scientific Laboratory (LASL), Ned Bibler of the Savannah River Laboratory (SRL), Doug Caldwell of the University of New Mexico (UNM), and Jeff Braithwaite of Sandia Laboratories in preparing this document and in interpretation of the data is greatly appreciated. A large fraction of their data and analyses, directly supported as portions of the WIPP TRU waste characterization program, have been incorporated directly.

GAS GENERATION FROM TRANSURANIC WASTE DEGRADATION:
DATA SUMMARY AND INTERPRETATION

Martin A. Molecke

1.0 INTRODUCTION

The generation of gases from the degradation of existing and potential forms of defense-related transuranic wastes has been the subject of extensive experimental investigations (1,2,3,4,5,6) over the past two to four years. This area of study, particularly under environmental conditions to be expected for deep geologic terminal isolation, is a major segment of the Waste Isolation Pilot Plant (WIPP) Transuranic (TRU) Waste Experimental Characterization Program. This program, conducted by Sandia Laboratories and sponsored by the Department of Energy, is summarized in detail elsewhere (1).

This paper summarizes and provides interpretation of all applicable waste degradation-gas generation data. This is an updated and significantly expanded review of an interim assessment document presented in January, 1979 (7). For completeness, data presented earlier (7) will be included along with the significant body of new data gathered in the last six months. This review and assessment has been compiled to assist the Department of Energy Waste Acceptance Criteria Steering Committee (WACSC) on their deliberations of acceptable TRU waste forms, whether existing in temporary storage or in laboratory development, for safe isolation in the WIPP.

This comprehensive review includes data on gas generation rates from several common TRU waste forms, various degradation mechanisms, synergism between mechanisms, resultant gas compositions, methods for reducing gas production rates, and comparisons between generation modes. Many of the experimental investigations to be described are still in progress; some of the data are preliminary and may be subsequently refined.

The mechanisms of TRU waste matrix and container degradation which result in gas generation are summarized in Table 1. Also listed are the major gases produced, in approximate order of abundance and significance.

The descriptions of radiolytic and bacterial degradation of organic waste matrices (Sections 2.0 and 4.0, respectively) have been significantly expanded since the previous interim assessment (7). Radiolytic degradation was initially assumed by the waste management community to have the greatest potential for generating significant quantities of gas. It has received the greatest amount of experimental attention (2,3,4,5,6) for this reason, and consequently, accounts for the largest body of data. Within approximately the last six months, it has become evident (7) that the bacterial degradation of organic waste matrices has a significantly greater potential for gas generation. Studies on bacterial degradation (8,9) are therefore described here in detail.

TABLE 1

GAS GENERATION FROM TRU WASTES

Mechanisms of Waste Degradation, Gas Production:

1. Radiolysis
2. Thermal Decomposition and Dewatering
3. Chemical Corrosion
4. Bacterial

Primary Gases Produced:

H₂, CO₂, CO, H₂O, CH₄, O₂, NO_x, He

Concerns of Gas Generation:

Long-term: pressurization of repository
breach in containment integrity

Operational Phase:

flammable, explosive, toxic concentrations of gases
fuel for fire, with initiating event
particulate contamination carrier
effects on mine design, operation

Areas of WIPP Study:

1. kinetics, species, total extent of gas generation
2. predictive analytical modeling of gas generation
3. techniques, additives for reducing generation rates
4. gas accumulation analysis
5. permeability studies on gas dissipation
6. mine response to gas accumulation
7. WIPP TRU waste acceptance criteria; to limit gas generation

The specific overall study areas for WIPP TRU waste characterization pertaining to gas generation and their significance are listed at the bottom of Table 1. The first three topics will be discussed herein. Output data from these endeavors are the input data for the mathematical in-mine gas accumulation analysis. Coupled with the laboratory and in situ measurements of rocksalt permeability to gases, analyses of the WIPP mine response to gas accumulation and pressurization can be conducted. These topics are reviewed elsewhere (10,11). All six of these study areas may have a combined, significant impact on the acceptability of various existing and potential TRU waste forms into the WIPP for long-term isolation. All these studies are in progress at Sandia Laboratories and contractor facilities.

The specific concerns about gas generation from TRU waste degradation and its potential impact on the WIPP, listed in Table 1, have been described previously (1,7).

1.1 WIPP Environmental Conditions

A general layout of the WIPP TRU repository is described elsewhere (11). Assessment of the conditions which could be present at the TRU waste storage horizon yields the following environmental conditions:

Temperature

Temperatures of interest for WIPP-specific studies of waste degradation range from 25°C (approximate WIPP mine ambient temperature during its operational phase) up to 100°C, for overtest purposes. While many of the conditions given here could not occur with the current WIPP configuration, conditions are postulated for more severe environments so that conservatism is maintained and the results may have more generic application.

If heat-generating wastes (e.g., high-level wastes) are considered present at the lower horizon of the WIPP at a thermal density of 75 kW/acre (18.5 watts/m²), the calculated maximum temperature obtained at the upper TRU horizon will be 43°C (12). The temperature will rise rapidly from ambient, reach its maximum at approximately 200 years (after sealing), then decrease slowly. This temperature versus time profile for the WIPP contact-handled TRU waste horizon is illustrated in Figure 1. The regional thermal analysis model used to calculate these results is illustrated in Figure 2. This indicates the general geologic strata at the WIPP site in southeastern New Mexico, the upper TRU waste horizon, and the lower horizon containing heat-generating wastes. An upper boundary temperature of 70°C was also investigated to assess the impact of higher thermal power densities or collocation of contact-handled TRU and heat-generating waste on the same repository horizon.

For experimental expediency, laboratory analyses are being conducted at 20° to 25°, 40°, 70°, and 100°C.

FIGURE 1

WIPP TRU CH LEVEL TEMPERATURE

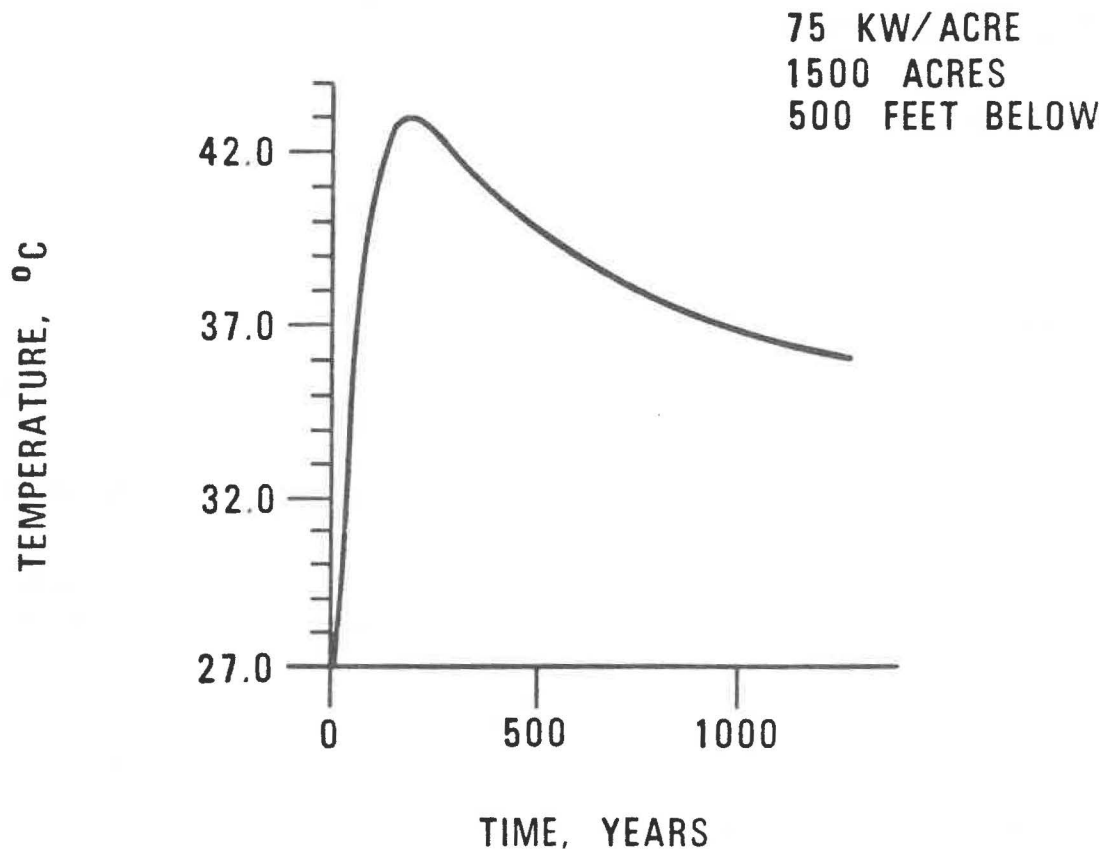
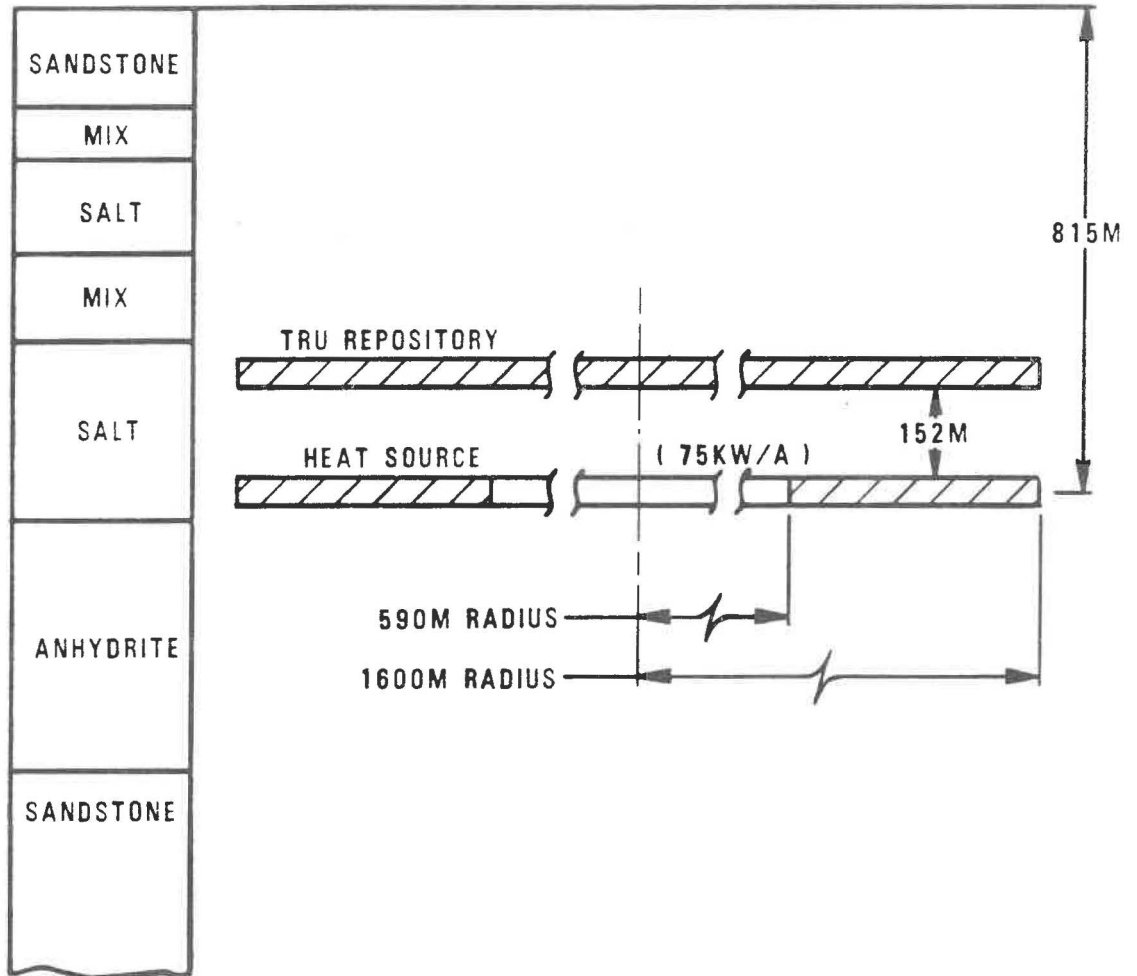


FIGURE 2

REGIONAL THERMAL ANALYSIS MODEL



Pressure

The pressure range of interest for experimental studies ranges from 0.1 to 15 MPa (1-150 atmospheres, 15-2100 psi). The lower pressure is the ambient pressure during the operational phase of the WIPP. The higher pressure is representative of lithostatic (rock overburden) pressure of the sealed repository at the 640 m (2100 ft) contact-handled TRU horizon.

Other

Prior to a breach in the waste container (which may not occur for at least several hundred years), waste degradation occurs in a non-salt, "in-can" environment. Other variables which may influence waste form degradation and gas generation rates, such as bedded salt chemistry/geochemistry, or the presence or absence of air atmosphere, will be described where applicable.

1.2 Waste Form Characteristics

The TRU-contaminated waste matrices of primary interest for the WIPP TRU waste characterization program (1) consist of: cellulose (paper, cotton, cloth, wood, etc), plastics (polyethylene, polyvinyl chloride), rubbers (neoprene, Hypalon), a composite organic matrix of the above components, concrete-TRU ash, process sludges, and asphalt. These wastes are usually contained in 210 liter (55 gallon) mild steel drums.

Characterization of existing TRU wastes in temporary storage have been conducted by Shefelbine for wastes at the Idaho National Engineering Laboratory, and by Barraclough (2,14), for similar wastes at the Los Alamos Scientific Laboratory.

For the earlier assessment of TRU waste degradation (7), a standard waste unit weight of 150 kg and a standard contamination level of 10 g, 0.77 alpha Ci, of weapons grade Pu (²³⁹Pu, primarily ²³⁹Pu) per drum were utilized for comparative purposes.

Comparison of gas generation rates versus degradation mechanism for representative, realistic TRU waste matrices will, in this summary, be based on a standard unit--the volume (and content) of a 210 liter drum.

For this report, waste definitions are modified to more closely represent individual waste types in existing temporary storage at INEL (13).

Weight

The average weight of 210 liter drums of all TRU waste types stored at INEL from September 1971 through December 1976 (13) is approximately 150 kg. However, 44 percent of these drums weigh less than 91 kg (gross), and of these, almost 80 percent contain organic waste forms such as paper, rags, and plastics (12). These are materials of prime degradation and gas generation concern. The average net weight of organic materials in the INEL-stored drums is 60 kg. The internal 2.4 mm (100 mil) high-density, 100 percent cross-linked polyethylene liner in the drums weighs 8.6 kg, resulting in an average TRU-contaminated organic waste matrix of 51.4 kg.

Other types of stored waste drums weigh between 180 and 270 kg, significantly skewing the weight distribution. Over 70 percent of the wastes within this range contain process sludges of various types (13); these sludges originate in large part from the plutonium recovery operations at the Rocky Flats Plant. Process sludges comprise approximately 21 percent by weight or 11 percent by volume of the pad stored TRU wastes at Idaho. They also contain approximately 60-70 percent by weight of sorbed water; as such, they are a matrix of significant concern for radiolytic gas generation and thermal water vapor release under representative repository environmental conditions. This latter aspect is discussed elsewhere (11).

Contamination

The actinide contamination level per drum is based on the average alpha activity contamination for each waste type in existing storage. The maximum permissible amount of alpha activity per 210-liter drum is 15 Ci, corresponding to 200 g of weapon grade Pu (1). However, extremely few drums of existing defense-related TRU waste actually approach this level. Of the waste drums stored in Idaho from September 1971, through December 1977, 94 percent contain 10 g or less of ^{wg}Pu , 78 percent contain 1 g or less, and 55 percent contain 0.5 g or less (12). The calculated average contamination for the organic, cellulosic wastes (both dry and wet) is only 0.29 g ^{wg}Pu /drum; for purposes of intercomparison, a contamination level of 0.5 g of ^{wg}Pu , or 0.039 alpha Ci per drum has been (conservatively) assumed for further calculations.

Other existing forms of TRU waste can contain significantly more contamination per drum. Existing first stage process sludge contains an average of 0.39 Ci per drum due to ^{wg}Pu , plus 6.5 Ci per drum due to ^{241}Am . This alpha activity is equivalent to 89 g ^{wg}Pu per drum! Approximately 17 percent of the total plutonium content of wastes, stored at Idaho is contained in this first stage sludge (12).

Developmental TRU waste matrices such as concrete-TRU ash or glass could be fully loaded to contain 200 g of weapons grade plutonium.

Table 2 briefly summarizes the representative TRU waste weights and contamination levels referred to throughout the rest of this document. Further details about individual waste types will be described where appropriate.

TABLE 2

ASSUMED CHARACTERISTICS OF STANDARD DRUM (210 liter) CONTENT

<u>Waste Material</u>	<u>Matrix Weight</u> (kg)	<u>Contamination</u> (g ^w gPu/Ci)
cellulosics	51.4	0.5/0.039
plastics	51.4	0.5/0.039
rubbers	51.4	0.5/0.039
organic composite	51.4	0.5/0.039
organic set-ups (solidified oils)	190	0.5/0.039
process sludges (first stage)	190	(89)/6.9
polyethylene liner	8.6	
mild steel drum	25	
concrete-TRU ash	300	200/15.4
asphalt	135	100/7.7

2.0 RADIOLYTIC DEGRADATION DATA

A summary of all known data on the gas generation rates of TRU wastes via radiolytic degradation is presented in Table 3. Values listed are in terms of moles (total gas)/year/drum produced and also in terms of G(total gas). Specifications for defined, comparative drum characteristics (e.g., matrix weight, contamination level) of existing or potential wastes were listed in Table 2.

G(gas) is defined as the number of gas molecules formed for each 100eV of irradiation; it is not a rate. For example, if G(gas) = 1.0, each alpha decay of ^{239}Pu (5.1 MeV) would yield 5.1×10^4 resultant gas molecules. G(gas) should not be considered (2) to be an intrinsic property of the material studied; it may, for example, be a function of the intimacy of contact between the waste matrix and the TRU contaminant. The specification of "total gas" means the overall production of all gas product molecules such as H_2 , CO_2 , etc., including the depletion of some molecules, such as O_2 . This will be elaborated on in subsequent sections.

Based on the definition of G(gas), the number of moles of gas produced per year per drum (the gas generation rate) can be calculated with the following equation:

$$\text{Moles of gas/year/drum} = (0.099 \text{ moles}) (\text{Ggas}) (\text{Ci/drum})$$

This simple equation does not include any possible effects of pressure, temperature, or dose rate dependency on the gas generation rate. It assumes all alpha decay energy is deposited in the waste matrix. This equation is used, disregarding its shortcomings, to convert the measured G(gas) values in Table 3 to gas production rates.

The most extensive investigations of radiolytic degradation of transuranic contaminated wastes have been conducted at LASL. Two parallel programs are in progress:

1. The S-124 program, funded by Sandia Laboratories as part of the WIPP TRU waste characterization program (1), is specific to WIPP environmental conditions of temperature, pressure, contamination, etc., as well as overtest conditions. This program has been in progress since October, 1977. Many of the data and conclusions in this section originate from this laboratory study.
2. The A-412 program (3) has been in progress for over four years and is sponsored by the waste management division (H-7) of LASL. Many of the data of this program, laboratory and field, corroborate similar work of the S-124 program.

A significant body of related data has also been generated at SRL. Some of the SRL studies have been funded by Sandia for the WIPP (5,15,16); some have not (4). Additional radiolytic degradation data have been gathered at the Rocky Flats Plant (RFP)(6).

TABLE 3

RADIOLYTIC DEGRADATION DATA SUMMARYTRU WASTE CONTAMINATED MATRICES

	<u>Matrix*</u>	<u>G (gas, total)</u>	<u>Moles/yr/drum**</u>	<u>Ref.</u>
LASL:	cellulosics	2.9-1.3	0.011-0.0050	14
	PVC	8-11	0.030-0.042	2
	asphalt	0.2-1.0	0.15-0.76	14
	cellulosics, dry	1.6	0.0061	3
	cellulosics, soaked	1.5	0.0057	3
	composite	1.4	0.0053	3
	polyethylene	1.9	0.0072	3
	pump oil	1.3-1.8	0.0050-0.0069	3
SRL:	cellulosics	1.9	0.0072	4
	pump oil	2.0	0.0076	4
	octane	4.5	0.017	4
	concrete TRU ash	0.0003-0.6	0.0005-0.93	16
RFP:	cellulosics (dry)	(0.63)	(0.0024)	6
	cellulosics (wet)	(0.31)	(0.0012)	6
	polyethylene	(0.73)	(0.0028)	6
	PVC	(0.43-0.96)	(0.0016-0.0037)	6
	plexiglas	(1.9)	(0.0072)	6
	rubbers	(0.37)	(0.0014)	6
	oil	(3.1)	(0.012)	6
	IX resins	(0.11)	(0.004)	6
	cemented resins	-	(0.99)- 15Ci	26
	production wastes	-	(0.002)- 0.039Ci	25
	(resins and wet combustibles)			
Alpha Decay:				
	He generation (0.5g ^w gPu)		3.7x10 ⁻⁸	
	(200g ^w gPu)		1.5x10 ⁻⁵	
	First Stage Process	1.0	0.7	
	Sludges			

*average content of ^wgPu per drum listed in Table 2

**two significant figures, maximum

July, 1979

A preliminary comparison of the measured G(gas) values reported by LASL (2,3,14), SRL (4), and RFP (6) can be made. The LASL and SRL values on cellulose and pump oil are quite comparable, the RFP values are not. The LASL and RFP values for other organic matrices also do not correspond. The probable reasons for these discrepancies will be discussed in the next several sections of this paper.

The LASL studies (14,17) have investigated radiolytic degradation and resultant gas generation as a function of the following variables:

1. Waste form--cellulosics (cotton and paper--dry, moist), polyethylene, PVC, composite (35 percent cellulose, 23 percent polyethylene, 12 percent PVC, 15 percent neoprene, 15 percent Hypalon rubber), asphalt, etc.
2. Pu contamination level/drum loading/dose rate - expressed as:
20 to 32,000g ^wG_{Pu}/drum, or
1.54 to 2464 alpha Ci/drum, or
0.1X - 160X (where X = 200g ^wG_{Pu}/drum)
3. Temperature - 20°C, 40°C, 70°C, and 100°C
4. Time - up to 480 days (14); more than 4 years (3)
5. Pressure - 0.1 to 15 MPa (1-150 atmospheres, 15-2100 psi)

The effects of these variables on gas generation will be described individually.

2.1 Dose Rate and Time Effects

In the past, alpha radiolysis degradation studies have been conducted at high dose rates with the assumption that dose rate had little or no resultant effect on measured G values. An obvious advantage (14) to using high dose rates is that data can be generated quickly and contributions to gas production from other degradation mechanisms, such as thermal or bacterial, will be greatly minimized. Based on recent data obtained at LASL by Kosiewicz (14), the appropriateness of linearly extrapolating high dose rate data and short observation times to realistic, low dose rate situations (existing TRU wastes) and long times should be carefully considered.

The dose rates used at LASL (14) ranged over a factor of 1600, from 0.4 - 640x10⁵ nCi/g of waste. At the dose rates investigated, G(gas) decreased as the elapsed time or integrated dose increased (14). This is attributed to localized organic matrix material depletion adjacent to the Pu contaminant material (3,14), or to the formation of degradation products that produce less gas as the irradiation progresses (4). The LASL data (2,3) were numerically fitted to a simple regression formula of the type:

$$G(\text{gas}) = C_1 \exp(-C_2 t)$$

where t is the elapsed time in days. When t = 0, then G(gas) = G⁰(gas).

A graph of G(gas) vs elapsed time, for cellulose at a 40X dose rate, was presented earlier (2,7). Similar curves for cellulose - wet and dry, organic composite, polyethylene, and pump oil, for an elapsed time of over four years, are presented elsewhere (3).

For an average Pu loading of less than 1 g/drum for existing TRU-contaminated organic composites at INEL (13), the decrease of G(gas) would be approximately three orders of magnitude slower than those wastes doped to 40X. The radiolytic gas generation rate for existing organic matrix TRU wastes, if isolated in the WIPP, would probably be quite constant for hundreds of years.

Experimentally determined G(gas) values for cellulose degradation were plotted versus integrated dose, for multiple dose rates, in Figure 3 (2), to determine $G^0(\text{gas})$. (For reference, the dose rate from 20g of ^{239}Pu per drum of waste, 0.1X, 1.54Ci, corresponds to $0.25 \times 10^{23} \text{eV/day}$ or $4.2 \times 10^{17} \text{eV/day/g}$ of waste in a 60 kg matrix.) For dose rates of less than or equal to 40X, $G^0(\text{gas})$ is 2.9 for cellulose (2). For dose rates of 80X and 160X, $G^0(\text{gas})$ apparently is 1.3 (2). The tentative explanation for this apparent anomaly is that there is a sharp, fast decrease in the curve for high dose rate samples that was not experimentally observed with periodic sampling. This is now being investigated (14). G(gas) initial values determined from the LASL data (3,14) and presented in Table 3 should be considered as upper limit values for the radiolytic gas generation from TRU wastes.

The effect of dose rate on $G(\text{H}_2)$ in concrete-TRU ash matrices was investigated at SRL (5,15,16) and will be described later. In the limited range of $0.14 - 1.4 \times 10^{20} \text{eV/day/g}$ of waste, no major effect was noticed in $G(\text{H}_2)$ for the concrete systems evaluated.

At Rocky Flats, Kazanjian (6) contaminated various common organic waste materials with either $^{239}\text{PuO}_2$ (2-20 micrometer particles) or $^{238}\text{PuO}_2$ (less than 30 micrometer particles). Contamination dose rates varying by up to a factor of 50 were utilized. He also noticed a decrease in gas generation rates as a function of time due to localized matrix depletion. Kazanjian postulated that depletion rates were dependent on contaminant particle size, with depletion times increasing as particle size decreases. Work by Bibler (5) with TRU-contaminated concretes came to exactly the opposite conclusion regarding particle size. It appears probable that the lower G(gas) values determined by Kazanjian (listed in Table 3) resulted from not extrapolating measured G(gas) values back to time $t = 0$, and instead selecting data after measurable waste depletion had occurred. The radiolysis data in Table 3 from RFP are enclosed in parentheses to indicate this uncertainty.

These experiments emphasize that care must be exercised when using high dose rate experiments and extrapolating back to actual TRU waste contamination conditions.

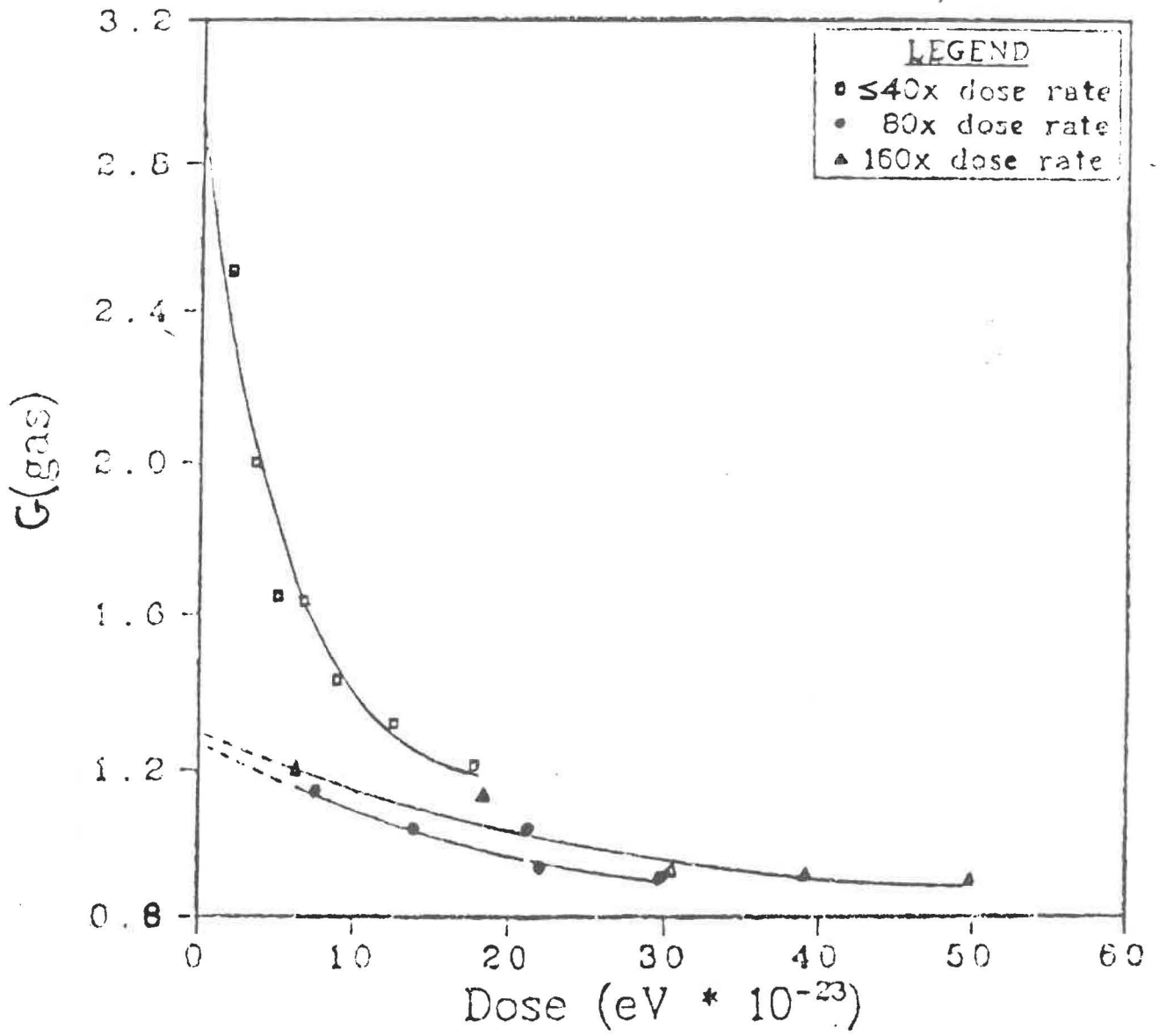


FIGURE 3
CELLULOSIC G(gas) VALUES VS INTEGRATED DOSE

2.2 Pressure Effects

The effects of gas generation from TRU waste degradation are of major significance with respect to how much gas is generated and what the effects or consequences of gas accumulation and potential pressurization (11) are on the sealed WIPP repository. Conversely, the effects of system pressurization on the rates of subsequent gas generation by various mechanisms are also a topic of interest. The effects of pressure on gas generation, e.g., whether rates are decreased and back reactions initiated yielding lesser quantities of resultant gas, are being investigated at LASL (2,3,14).

Three experimental techniques are being utilized (2):

1. Cylinders containing highly doped organic matrices are sealed in an instrumented cylinder, then initially pressurized to 10 MPa (1500 psi) with deuterium gas. This technique is similar to, but more rapid than, technique #2.
2. Highly doped (160X) organic matrices are sealed in an instrumented cylinder and allowed to self-pressurize. Pressures of several MPa (several hundred psi) should occur in less than a year.
3. A polyurethane liner is crushed (with Ar gas) against a contaminated waste matrix at WIPP lithostatic pressure. This investigates whether crushing the matrix increases the contact efficiency between it and the plutonium contaminant, with a subsequent change in radiolytic gas production.

For technique #1, for both cellulose and polyethylene, the observed rate of hydrogen evolution appears to have decreased 50-60 percent; after four months, no (or very little) pressure increases have been observed (14). The observed decreases may be the result of:

- a. suppression of additional hydrogen formation by the initial high deuterium pressure,
- b. recombination of deuterium with the matrix while hydrogen is still being produced, resulting in a decreased gas generation, or
- c. very small leaks out of the highly pressurized cylinder; comparable cellulosic and polyethylene matrix test results rule against this option.

Mass spectrometric analysis of the gases produced (2) suggest that option b above is probably correct. Option c above, however, cannot be totally discounted yet; analysis is continuing.

For technique #2, self-pressurization, pressures of 1 MPa (150 psi) have been achieved. Comparison with low-pressure experiments indicates that the generation rate is decreasing as the pressure in the test cylinder increases (14); observation is continuing.

Zerwekh (3) corroborated most of the above observations in a similar series of experiments. He measured the pressure increase of ^{238}Pu contaminated cellulose allowed to self-pressurize to 690 kPa (100 psi), then sampled/depressurized, allowed to repressurize, etc., over a period of about four years. The results of this test were compared to a parallel test which was allowed to self-pressurize up to only 103 kPa (15 psi) sequentially. The rate of gas formation was clearly less (3) in the more highly pressurized cylinder; gas generation decreases as the pressure increases. In addition, water was repeatedly found in the 690 kPa cylinder, but not in the 103 kPa cylinder. The water was generated at a rate of 10.5 micrograms $\text{H}_2\text{O}/\text{year}/\text{gram}$ of cellulosic waste (at the contamination level utilized, 40X); for an average drum of cellulosic waste (Table 2), this is equivalent to about 34 micrograms $\text{H}_2\text{O}/\text{year}$, once sufficient pressure has accumulated. The data appear to indicate that the water formation is the result of recombination of H_2 and O_2 (from entrapped air). Recombination of hydrogen and oxygen at these pressures, however, remains somewhat questionable. Zerwekh concluded (3) that, as the waste system in a sealed repository attains relatively high pressure, the rate of gas (and water) production would decrease and become insignificant.

For an alpha-contaminated concrete matrix, Bibler (4) measured a linear increase (constant rate) in radiolytic gas production up to 1.4 MPa (200 psi).

For technique #3, the lithostatic matrix crushing experiment, the measured gas generation rate for this pressurized system was approximately one-third as large (for cellulose) as a similar non-pressurized system. Because of repeated experimental difficulties with this test cylinder, however, firm conclusions cannot be made. The series of tests using this technique has been discontinued.

2.3 Temperature Effects

Synergistic effects of temperature and alpha radiolysis on gas generation rates have been experimentally measured by Kosiewicz (2) and Zerwekh (3) for cellulose, and by Kazanjian and Horrell (18) for PVC. Bowmer and O'Donnell (19) found increases at higher temperatures in the gas yield of low-density polyethylene upon gamma irradiation. Turner (20) did not feel that moderate temperature changes could be expected to exert much influence on the radiation chemistry of polymers.

Zerwekh (3) measured the radiolytic degradation of cellulose at -13° , 20° , and 55°C . Between 20°C and 55°C , an increase of 43 percent for gas generation (corrected for standard temperature and pressure) was determined. With time, this synergistic effect became less pronounced and may cease to be important for long-term isolation.

For a temperature increase of 50° , between 20° and 70°C , Kosiewicz (14) found a corresponding increase in radiolytic gas generation of 70 percent. This increase diminished to about +30 percent after 71 days and has stabilized at approximately +30 percent out to 188 days. The disappearance of this synergistic effect may take a very long time; observation is continuing.

2.4 Composition of Radiolysis Gases

The gas composition from radiolysis of cellulose at 20°C was determined (2) to consist of 60 mole percent of H₂, with smaller amounts of CO₂, CO, and CH₄. The mole ratio H₂:CO₂:CO was calculated to be 1.0:0.43:0.22. A similar SRL analysis (4) on radiolytic cellulose degradation determined a similar ratio of 1.0:0.7:0.3. In both studies, oxygen originally in the test cylinder was depleted, probably having been consumed to form CO₂ and CO. At 55°C, Zerwekh (3) also detected a trace of organic gas with a molecular weight of 60. Degradation of polyethylene yielded about 95 percent hydrogen (2). Polyvinyl chloride (PVC) yields 90 percent H₂, 4.5 percent CO₂, and 4.5 percent CO (2); a small amount of CH₄ was also detected (14). No HCl (2,3) or Cl species (14) were detected by mass spectrometric analysis. The carbon oxide species probably resulted from reactions involving the initially present oxygen; this was supported by a second gas analysis (14). Hydrogen is also the major gas produced by the alpha radiolysis of asphalt (14).

The alpha radiolysis of water (21), a small constituent of TRU wastes, yields hydrogen and oxygen in a mole ratio of 88:12.

2.5 Field Test Data

LASL (3,22,23), SRL (24), and RFP (25,26) have each conducted field tests on gases generated in drums of production wastes, either measured in the field or brought back into the laboratory for analysis.

Zerwekh at LASL (3,22,23) periodically sampled drums of organic matrix wastes plus a large variety of mixed and non-organic TRU trash located in a trench at the LASL waste disposal area. Wastes were contaminated with either ²³⁸Pu or ²³⁹Pu. Gas samples were taken for compositional analyses, pressure was monitored inside and outside the drums, and temperatures were monitored inside, outside, and under the drums.

There was no practical way to measure the quantity of gases produced (3) because of diffusion through drum gaskets, cement shielding cask walls, and the earthen overburden. No significant internal drum pressurization was detected due to leakage through the drum gaskets; the gaskets are, however, liquid and particulate tight.

The measured gas compositions inside the instrumented drums are listed elsewhere (3). Several explosive gas mixtures were detected in ²³⁸Pu highly contaminated drums, some changed to non-explosive but combustible compositions after a period of time. H₂ concentrations increased with time and the O₂ was depleted as a result of CO₂ and CO formation. Hydrogen is explosive in air when present in the range of 4-76 volume percent. It was also determined (3) that oxygen (in air) could diffuse into the drums while H₂ diffused out. It was stated (22) that all ²³⁸Pu-contaminated drums in temporary storage should be considered potentially explosible until individual drum gas contents have been analyzed, vented, and/or replaced with an inert gas. McLain (27) also reported hydrogen concentrations greater than the minimum explosive mixture following exhumation

of culverts containing Pu-contaminated wastes after five years of burial. This should be of significant short-term concern when recovering, handling, or reprocessing stored TRU wastes.

At SRL (24), four typical Savannah River Plant waste drums and one waste culvert were monitored for radiogenic gas composition and internal pressurization. Such monitoring covered a period of about 700 days. Drum internal over-pressures of up to 4 psi were detected; the drum gaskets permitted H₂ and other gases to diffuse out while oxygen from the air diffused inward replacing some of the radiolytically depleted oxygen. Hydrogen concentrations in some of the drums approached 25 percent by volume; CO₂ similarly approached 20 percent by volume.

At RFP (25,26), the hydrogen production rate of several drums of contaminated production wastes was measured. The production wastes consisted of cemented ion exchange resins and cemented resins plus moist combustibles (including plastics and rubbers). "Cemented" ion exchange resins refers to layers of moist, organic ion exchange resins separated by layers of cement powder used to stabilize and soak up some of the moisture.

Taking the radiolytic degradation data available, Zerwekh (3) surmised that the amount of hydrogen produced from existing production wastes would, extrapolated to 20 years, exceed explosive limits in air in a closed/sealed TRU waste storage facility. This conjecture is being analyzed.

2.6 Concrete Matrix TRU Wastes

Previous studies at SRL (15,28) have investigated the radiolytic degradation and gas generation rate of defense high-level waste sludges incorporated into concrete matrices. Current studies (5,15,16) are focusing on the radiolytic gas generation of TRU waste ashes incorporated into a concrete matrix under conditions that such a waste form might encounter in the WIPP. If the decision is eventually made to incinerate (or slag, or digest) the combustible, organic segments of defense TRU waste currently held in temporary surface or shallow-trench storage, concrete may prove a viable encapsulating matrix for the resultant ashes (or other products).

The studies at SRL, funded by the WIPP project (1), are to determine the relative gas generation capacity of concretes vs. organic waste matrices. Studies are also designed to determine techniques or additives which could significantly reduce the gas generation rate of the concrete. A significant amount of data has been reported and will be summarized (4,5,15,16).

Cement types investigated at SRL include high alumina cement (HAC), portland type 1 cement (I), and portland type 1-pozzolanic cement (I-P). The TRU waste ash simulant was made by the incineration of common laboratory type waste (shoe covers, rubber gloves, cellulosic materials, polyethylene tubing, etc.); this ash was calcined at 800°C, yielding a low residual carbon content. The ash contains primarily CaO and TiO₂, with a much

smaller content of other oxides. A mixture of 30 weight percent ash in a dry cement mix gave suitable workability of the resultant concrete paste. After curing, the tested water:cement-plus-ash ratio was 0.3-0.4. ^{238}Pu plutonium contaminant was added either as a solution (in 0.2M H_2SO_4 , to keep the Pu in solution) to the water used to make the concrete, or as $^{238}\text{PuO}_2$ particles added to the dry mix.

A non-simulated TRU ash was also prepared by incinerating (at 900°C) laboratory waste contaminated with ^{238}Pu solution (16). This non-simulated ash was mixed with the simulated ash for doping the concrete.

Tests indicated that radiolysis produced H_2 and, depending on the method of making the concrete, O_2 . If the concrete was prepared as a monolith by using a removable mold, O_2 was not produced (5). If the concrete was cast and cured in a steel cylinder, O_2 was produced. The latter method probably is more representative of the preparation technique to be utilized if concrete-TRU ash matrix waste was to be produced, on a per-drum basis, for waste isolation.

The gas generation capacity of the doped concrete was determined in terms of $G(\text{H}_2)$ and $G(\text{total gas})$ values. G values were determined from both changes in the sample-system pressure and from the measured final gas composition and total dose. G values determined under various conditions for the concrete-TRU ash system are summarized in Tables 4a and 4b.

For the HAC, I, and I-P contaminated concretes cast as monoliths (in removable molds), H_2 was generally the only gas produced, O_2 was depleted, and N_2 was unaffected (deviations will be described). Hydrogen was not produced when concrete containing no Pu was heated to 70° and 100°C . Similarly, neither H_2 nor a pressure increase was detected when the non-simulated ^{238}Pu ash was sealed in a container and observed.

$G(\text{total gas})$ is, in most cases, the sum of $G(\text{H}_2)$ and $G(\text{O}_2)$, and to a very minor extent, $G(\text{N}_2\text{O})$. For the waste systems investigated in this study, $G(\text{O}_2)$ was either zero or negative. Oxygen is, of course, produced from oxidation of the O atoms in water. When O_2 is not formed, some other oxidized specie such as H_2O_2 must form. The reason for O_2 not being formed or detected when the concrete sample is cast as a monolith is not presently known. Perhaps some chemical compound that leached out of the removable plastic mold during sample preparation was reacting with radiolytically formed oxygen radicals, preventing O_2 formation. This could explain the observed O_2 depletion with cast monolith samples.

$G(\text{gas})$ values were higher (5,28) when the concrete contained the 30 percent simulated ash (with liquid Pu doping) than when it did not. $G(\text{gas})$ values with and without ash are 0.51 vs. 0.33, 0.55 vs. 0.48, and 0.73 vs. 0.51 for HAC, I, and I-P concrete matrices, respectively. (The I-P matrix was eliminated after this test.) The increase of $G(\text{gas})$ with ash present is due to the association of some water with the ash.

TABLE 4a

RADIOLYSIS DATA OF HIGH ALUMINA CONCRETE-TRU ASH SAMPLES

Cast as Monoliths (5 cm x 1.7 cm OD), Removable Mold

<u>Test condition:</u>	<u>T^oC</u> (+2 ^o C)	<u>G(H₂)</u>	<u>G(total gas)</u>
without ash, Pu(L), hdr	23	0.42	0.33
with ash, Pu(L), hdr	23	0.55	0.51
with ash, Pu(L), ldr	23	0.48	0.24
with ash, Pu(L), hdr	23	0.55	0.51
	70 sh	0.24	0.14
	70 hs	0.15	0.17
	100 hs	0.13	0.15
with ash, Pu(S) hdr			
non-heated (36% water)	23	0.21 ± 0.01	0.21 ± 0.03
heated at 200 ^o (17% water)	23	0.022	0.016
with ash, EDTA, Pu(L), hdr	23	0.30	0.15
	70 sh	0.19	---
	70 hs	0.06	0.04
with ash, 0.01M Fe(NO ₃) ₃ , Pu(L)	23	0.30	0.25
with ash, 1M Fe(NO ₃) ₃ , Pu(L)	23	0.08	0.43
with ash, 2M Fe(NO ₃) ₃ , Pu(L)	23	0.03	0.43
with ash, 0.3M NaNO ₂ , Pu(S)	23	0.15	0.14
with ash, 1M NaNO ₂ , Pu(S)	23	0.079	0.087
with ash, 3M NaNO ₂ , Pu(S)			
non-heated (36% water)	23	0.084	0.03
heated at 200 ^o (27% water)	23	0.031	0.023

Cast in Steel Canister (10cm x 2 cm ID)

with ash, Pu(S), hdr	23	0.28 ± 0.04	0.31 ± 0.01
non-simulated ash, ldr	23	0.29	0.30
heated at 90 ^o C (22% H ₂ O)	23	0.074	0.10
heated at 200 ^o (14% H ₂ O)	23	0.0005	N.D.

Note: Pu(L) = ²³⁸Pu in 0.2M H₂SO₄
 hdr = 10¹⁷ eV/min/g
 sh = sealed, then heated
 N.D. = not detected

Pu(S) = particulate ²³⁸PuO₂
 ldr = 10¹⁶ eV/min/g
 hs = heated, then sealed

TABLE 4b

RADIOLYSIS DATA OF PORTLAND TYPE I CONCRETE-TRU ASH SAMPLES

Cast as Monoliths (5 cm x 1.7 cm OD), Removable Mold

<u>Test condition:</u>	<u>T^oC</u> <u>(+2^oC)</u>	<u>G(H₂)</u>	<u>G(total gas)</u>
without ash, Pu(L), hdr	23	0.43	0.48
with ash, Pu(L), hdr	23	0.65	0.55
with ash, Pu(L), ldr	23	0.63	0.61
with ash, Pu(S), hdr	23	0.28	0.27
with ash, Pu(S), hdr	23	0.65	0.55
	70 sh	0.48	0.46
	70 hs	0.15	0.17
	100 hs	0.11	0.05
with ash, EDTA, Pu(L), hdr	23	0.35	0.05
	70 sh	0.31	0.29
	70 hs	0.08	0.07
	100 hs	0.05	0.03
with ash, 0.01M Fe(NO ₃) ₃ Pu(L)	23	0.34	0.31
with ash, 1M Fe(NO ₃) ₃ , Pu(L)	23	0.08	0.43
with ash, 2M Fe(NO ₃) ₃ , Pu(L)	23	0.03	0.16

Cast in Steel Canister (10cm x 2 cm ID)

with ash, Pu(S), hdr			
non-heated (30% H ₂ O)	23	0.32	0.49
heated at 90 ^o (28% H ₂ O)	23	0.20	0.30
heated at 100 ^o (8.2% H ₂ O)	23	0.009	N.D.
heated at 200 ^o (7.4% H ₂ O)	23	0.00029	N.D.

TABLE 4a

RADIOLYSIS DATA OF HIGH ALUMINA CONCRETE-TRU ASH SAMPLES

Cast as Monoliths (5 cm x 1.7 cm OD), Removable Mold

<u>Test condition:</u>	<u>T^oC</u> <u>(+2^oC)</u>	<u>G(H₂)</u>	<u>G(total gas)</u>
without ash, Pu(L), hdr	23	0.42	0.33
with ash, Pu(L), hdr	23	0.55	0.51
with ash, Pu(L), ldr	23	0.48	0.24
with ash, Pu(L), hdr	23	0.55	0.51
	70 sh	0.24	0.14
	70 hs	0.15	0.17
	100 hs	0.13	0.15
with ash, Pu(S) hdr			
non-heated (36% water)	23	0.21 ± 0.01	0.21 ± 0.03
heated at 200 ^o (17% water)	23	0.022	0.016
with ash, EDTA, Pu(L), hdr	23	0.30	0.15
	70 sh	0.19	---
	70 hs	0.06	0.04
with ash, 0.01M Fe(NO ₃) ₃ , Pu(L)	23	0.30	0.25
with ash, 1M Fe(NO ₃) ₃ , Pu(L)	23	0.08	0.43
with ash, 2M Fe(NO ₃) ₃ , Pu(L)	23	0.03	0.43
with ash, 0.3M NaNO ₂ , Pu(S)	23	0.15	0.14
with ash, 1M NaNO ₂ , Pu(S)	23	0.079	0.087
with ash, 3M NaNO ₂ , Pu(S)			
non-heated (36% water)	23	0.084	0.03
heated at 200 ^o (27% water)	23	0.031	0.023

Cast in Steel Canister (10cm x 2 cm ID)

with ash, Pu(S), hdr	23	0.28 ± 0.04	0.31 ± 0.01
non-simulated ash, ldr	23	0.29	0.30
heated at 90 ^o C (22% H ₂ O)	23	0.074	0.10
heated at 200 ^o (14% H ₂ O)	23	0.0005	N.D.

Note: Pu(L) = ²³⁸Pu in 0.2M H₂SO₄
 hdr = 10¹⁷ eV/min/g
 sh = sealed, then heated
 N.D. = not detected

Pu(S) = particulate ²³⁸PuO₂
 ldr = 10¹⁶ eV/min/g
 hs = heated, then sealed

TABLE 4b

RADIOLYSIS DATA OF PORTLAND TYPE I CONCRETE-TRU ASH SAMPLES

Cast as Monoliths (5 cm x 1.7 cm OD), Removable Mold

<u>Test condition:</u>	$T^{\circ}\text{C}$ ($+2^{\circ}\text{C}$)	$G(\text{H}_2)$	<u>G(total gas)</u>
without ash, Pu(L), hdr	23	0.43	0.48
with ash, Pu(L), hdr	23	0.65	0.55
with ash, Pu(L), ldr	23	0.63	0.61
with ash, Pu(S), hdr	23	0.28	0.27
with ash, Pu(S), hdr	23	0.65	0.55
	70 sh	0.48	0.46
	70 hs	0.15	0.17
	100 hs	0.11	0.05
with ash, EDTA, Pu(L), hdr	23	0.35	0.05
	70 sh	0.31	0.29
	70 hs	0.08	0.07
	100 hs	0.05	0.03
with ash, 0.01M $\text{Fe}(\text{NO}_3)_3$ Pu(L)	23	0.34	0.31
with ash, 1M $\text{Fe}(\text{NO}_3)_3$, Pu(L)	23	0.08	0.43
with ash, 2M $\text{Fe}(\text{NO}_3)_3$, Pu(L)	23	0.03	0.16

Cast in Steel Canister (10cm x 2 cm ID)

with ash, Pu(S), hdr			
non-heated (30% H_2O)	23	0.32	0.49
heated at 90° (28% H_2O)	23	0.20	0.30
heated at 100° (8.2% H_2O)	23	0.009	N.D.
heated at 200° (7.4% H_2O)	23	0.00029	N.D.

TABLE 4a

RADIOLYSIS DATA OF HIGH ALUMINA CONCRETE-TRU ASH SAMPLES

Cast as Monoliths (5 cm x 1.7 cm OD), Removable Mold

<u>Test condition:</u>	<u>T^oC</u> (+2 ^o C)	<u>G(H₂)</u>	<u>G(total gas)</u>
without ash, Pu(L), hdr	23	0.42	0.33
with ash, Pu(L), hdr	23	0.55	0.51
with ash, Pu(L), ldr	23	0.48	0.24
with ash, Pu(L), hdr	23	0.55	0.51
	70 sh	0.24	0.14
	70 hs	0.15	0.17
	100 hs	0.13	0.15
with ash, Pu(S) hdr			
non-heated (36% water)	23	0.21 ± 0.01	0.21 ± 0.03
heated at 200 ^o (17% water)	23	0.022	0.016
with ash, EDTA, Pu(L), hdr	23	0.30	0.15
	70 sh	0.19	---
	70 hs	0.06	0.04
with ash, 0.01M Fe(NO ₃) ₃ , Pu(L)	23	0.30	0.25
with ash, 1M Fe(NO ₃) ₃ , Pu(L)	23	0.08	0.43
with ash, 2M Fe(NO ₃) ₃ , Pu(L)	23	0.03	0.43
with ash, 0.3M NaNO ₂ , Pu(S)	23	0.15	0.14
with ash, 1M NaNO ₂ , Pu(S)	23	0.079	0.087
with ash, 3M NaNO ₂ , Pu(S)			
non-heated (36% water)	23	0.084	0.03
heated at 200 ^o (27% water)	23	0.031	0.023

Cast in Steel Canister (10cm x 2 cm ID)

with ash, Pu(S), hdr	23	0.28 ± 0.04	0.31 ± 0.01
non-simulated ash, ldr	23	0.29	0.30
heated at 90 ^o C (22% H ₂ O)	23	0.074	0.10
heated at 200 ^o (14% H ₂ O)	23	0.0005	N.D.

Note: Pu(L) = ²³⁸Pu in 0.2M H₂SO₄
 hdr = 10¹⁷ eV/min/g
 sh = sealed, then heated
 N.D. = not detected

Pu(S) = particulate ²³⁸PuO₂
 ldr = 10¹⁶ eV/min/g
 hs = heated, then sealed

TABLE 4b

RADIOLYSIS DATA OF PORTLAND TYPE I CONCRETE-TRU ASH SAMPLES

Cast as Monoliths (5 cm x 1.7 cm OD), Removable Mold

<u>Test condition:</u>	$T^{\circ}\text{C}$ ($+2^{\circ}\text{C}$)	$G(\text{H}_2)$	<u>G(total gas)</u>
without ash, Pu(L), hdr	23	0.43	0.48
with ash, Pu(L), hdr	23	0.65	0.55
with ash, Pu(L), ldr	23	0.63	0.61
with ash, Pu(S), hdr	23	0.28	0.27
with ash, Pu(S), hdr	23	0.65	0.55
	70 sh	0.48	0.46
	70 hs	0.15	0.17
	100 hs	0.11	0.05
with ash, EDTA, Pu(L), hdr	23	0.35	0.05
	70 sh	0.31	0.29
	70 hs	0.08	0.07
	100 hs	0.05	0.03
with ash, 0.01M $\text{Fe}(\text{NO}_3)_3$ Pu(L)	23	0.34	0.31
with ash, 1M $\text{Fe}(\text{NO}_3)_3$, Pu(L)	23	0.08	0.43
with ash, 2M $\text{Fe}(\text{NO}_3)_3$, Pu(L)	23	0.03	0.16

Cast in Steel Canister (10cm x 2 cm ID)

with ash, Pu(S), hdr			
non-heated (30% H_2O)	23	0.32	0.49
heated at 90° (28% H_2O)	23	0.20	0.30
heated at 100° (8.2% H_2O)	23	0.009	N.D.
heated at 200° (7.4% H_2O)	23	0.00029	N.D.

The G(gas) value was lower (5) by approximately a factor of 2 when the ^{238}Pu was added as solid PuO_2 particles rather than being dissolved in H_2O to make the concrete. G(gas) of Pu(solution) vs. Pu(solid) are: 0.51 vs. 0.21, and 0.55 vs 0.27 for HAC and I concretes, respectively. This reduction resulted (5) from some of the alpha energy being absorbed in the PuO_2 particle rather than in H_2O , yielding H_2 . The range of an alpha particle in concrete is only about 0.01 mm. When the non-simulated ash was added to the HAC matrix, results indicated (16) that the form of the Pu, whether it was added as PuO_2 or whether it resulted from the incineration of Pu-contaminated combustibles, had no major effect. The G(gas) values for the non-simulated and solid PuO_2 doped matrices are 0.30 and 0.21, respectively. The difference could indicate (16) that the ^{238}Pu is in a less dense form in the incinerated ash than in the PuO_2 doped ash simulant. More of the energy of the alpha particles would then be available to reduce water to hydrogen. The non-simulated incinerated ash plus concrete sample results should be quite representative of actual TRU waste produced in this manner.

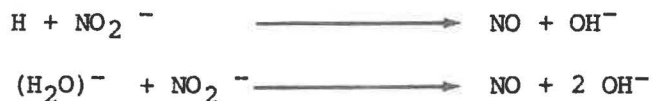
A zero-order rate dependency was determined (5,28) for $G(\text{H}_2)$ in the concrete matrices studied. This is somewhat different from the dose rate dependency determined for organic waste matrices, described in Section 2.1. The dose rates utilized at SRL ranged from 10^{16} - 10^{17} eV/min/g of concrete. A maximum drum loading of 200g ^{238}Pu corresponds to 5.8×10^{14} eV/min/g of concrete (in 300 kg of concrete). A reasonable mechanism for H_2 formation from radiolysis of water in concrete is recombination of H atoms, similar to that occurring in the radiolysis of liquid water (29). If this is the case, no dose rate effect at lower dose rates would be predicted. However, confirmation of this requires further testing.

The G(gas) value of concrete-TRU ash waste can be significantly decreased by the addition of scavenging agents which react with the precursors of H_2 . Scavengers investigated include nitrate and nitrite ions and EDTA. The organic complexing agent, 0.03M EDTA, was dropped after preliminary tests because it could be responsible for enhanced actinide mobility if the wastes are leached.

Both nitrate and nitrite ions reduce $G(\text{H}_2)$ by reacting with the precursors of H_2 . In liquid water these precursors are H atoms and solvated electrons, $(\text{H}_2\text{O})^-$. The scavenging reactions for nitrate ions are:



The scavenging reactions for nitrite ions are:



The scavenging reactions prevent the following:



Tests were run with 0.01-2M $\text{Fe}(\text{NO}_3)_3$ solutions. This compound was chosen because Fe^{+3} ions also have the ability of reacting with precursors of H_2 . The $\text{Fe}(\text{NO}_3)_3$ reduced $G(\text{H}_2)$ by a factor of about 20. However, oxygen was produced at a significant rate, $G(\text{O}_2) = 0.31-0.35$; the O_2 results from the radiolytic reduction of NO_3^- . The overall reduction of $G(\text{gas}) = G(\text{H}_2) + G(\text{O}_2)$ ranged from about 16 percent for HAC to over 300 percent for type I concrete.

A 0.3-3M NaNO_2 solution was added with the particulate PuO_2 contaminant as a scavenger. The nitrite ion is not stable in acid solution. Nitrite ions are less effective than nitrate ions for reducing $G(\text{H}_2)$, but are more effective for reducing the overall $G(\text{gas})$ value. For HAC, the nitrite reduces $G(\text{gas})$ from 0.3 ± 0.1 down to 0.03. The NO formed with nitrite additions could then react with O_2 to form NO_2 ; this would account for the observed oxygen depletion with this system. The NO_2 formed in the presence of both nitrite and nitrate ions could then react with H_2O to form more NO_3^- ions. NO_2 gas was observed experimentally. There is no a priori reason why these scavenging reactions could not occur in water solidified by cement matrices.

It was also determined (15) that changing the pH of added water (containing contaminant with an organic complexant agent) from 0.6 to 7 did not significantly alter $G(\text{H}_2)$. This is consistent with the fact that $G(\text{H}_2)$ is independent of pH for liquid water (29).

For the HAC matrix, $G(\text{gas})$ was not significantly affected (5) by temperature in the range of $23^\circ-70^\circ\text{C}$. For the I matrix, $G(\text{total})$ decreased by a factor of up to 12 at temperatures up to 100°C ; this resulted from the loss of free water from the concrete rather than from the increase in temperature. Tests at 70° and 100°C showed that $G(\text{gas})$ was essentially independent of temperature for concretes that had about the same water content.

2.6.1 Effect of Dewatering (16):

Because hydrogen results from radiolysis of water, removal of water from the concrete should lower the rate of H_2 production. In the extreme, if no water were present, no H_2 would be produced. To test this hypothesis, concretes were heated, after an initial radiolysis test and determination of $G(\text{H}_2)$, to remove some of the water. $G(\text{H}_2)$ was then redetermined. Results indicated that $G(\text{H}_2)$ could be reduced significantly (factors ranging from 3 to 30) by heating for 16 hours at 100 or 200°C . Most of the water in concrete is added to achieve a workable paste that can be poured or cast, rather than to cause the hydration reactions that give concrete its strength (30). Consequently, removal of water by heating at temperatures up to 200°C after the concrete has cured does not severely affect its strength (31).

Three different compositions of concrete were used to test the effect of dewatering: portland type-I concrete, high-alumina concrete, and high-alumina concrete containing nitrite ions as a scavenging agent.

Measured G values for the heated samples are presented in Tables 4a and 4b. $G(H_2)$ and $G(\text{total})$ were reduced in all cases, resulting in the lowest values obtained in this study. The drastic reduction in gas generation/pressurization potential caused by dewatering is illustrated in Figures 4a, b, c. The effect is least evident when nitrite is present because the generation rate has already been reduced by nitrite ions scavenging the precursors of H_2 and by causing O_2 depletion.

The greatest reduction in $G(H_2)$ was with portland type-I concrete because the water content of this concrete after heating was the lowest, about 8 percent residual water.

The HAC concrete containing nitrite ions generated a small amount of N_2O gas, having a $G(N_2O)$ value of 0.03, whether heated or not. Heating had no effect on the amount of nitrite ions present.

The decreases in $G(H_2)$ and $G(\text{total})$ are much greater than can be accounted for by the decrease in the water content of the concrete. If $G(H_2)$ depended only on the amount of water present, then decreasing this amount by a certain factor should decrease $G(H_2)$ by the same factor. The measured data indicate that this is not the case. With portland type-I concrete, the amount of water present decreased by a factor of 4.8 while $G(H_2)$ decreased by a factor of 36. Similarly, for the high-alumina concrete not containing nitrite ions, the amount of water decreased by a factor of 1.9 while $G(H_2)$ decreased by a factor of 10. When nitrite ions were present, the amount of water decreased by a factor of 1.5 while $G(H_2)$ decreased by a factor of 2.7.

The large relative decreases in $G(H_2)$ indicate (5) that the water remaining in the concrete is less susceptible to radiolytic reduction, leading to H_2 production, than is the water that was evolved from the concrete due to heating. The water that evolved was probably free water sorbed onto the concrete, while that remaining may be incorporated into the hydration products of the cement. This latter type of water may be able to transfer absorbed energy to the oxides of the concrete and thus not dissociate and lead to H_2 formation.

Upcoming studies at SRL will measure changes in $G(H_2)$ and $G(\text{total gas})$ produced by rewetting concrete previously heated, as described above. This should simulate a credible water intrusion scenario into a TRU waste repository.

2.6.2 Pressed Concrete Radiolysis:

For the past several months, gas measurements have also been conducted at SRL on pressed concrete pellets, containing TRU incinerator ash, that were produced at Mound Laboratory (32). These pellets of cement-ash paste are pressed at 25000 psi and nominally contain less than 3 weight percent of water compared to about 30 weight percent in cast concrete. Another advantage of this concrete is that it can hold up to 70 weight percent ash without adversely affecting the compressive strength of the final product (pellets, 1.2 cm OD by 1.2 cm).

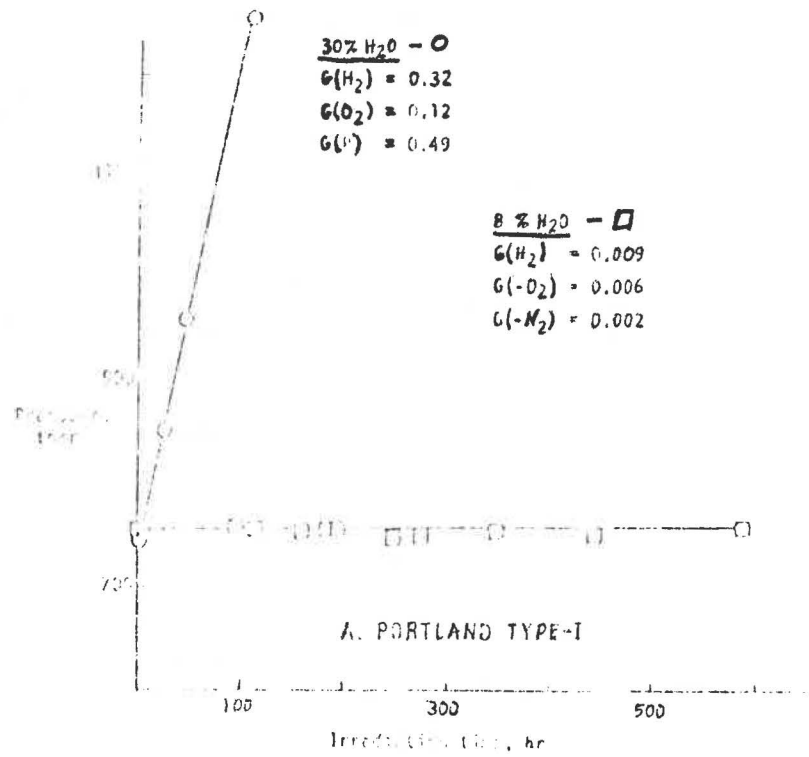
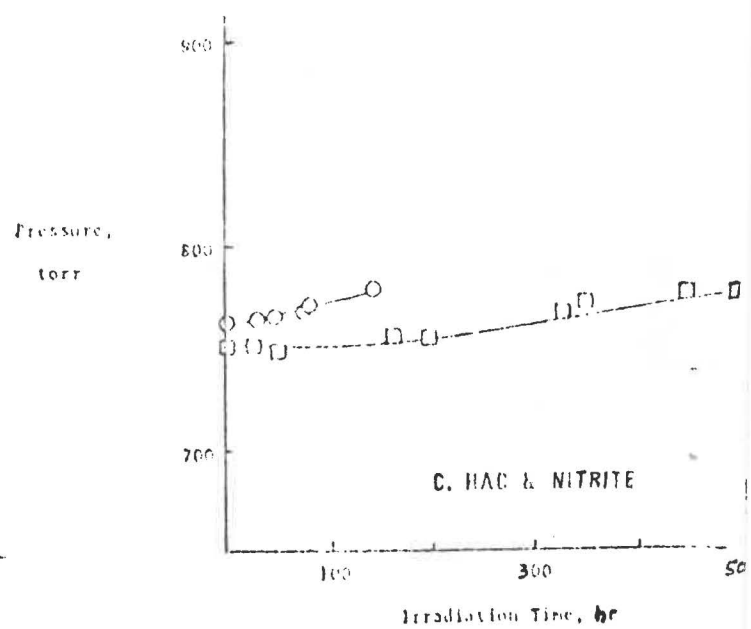
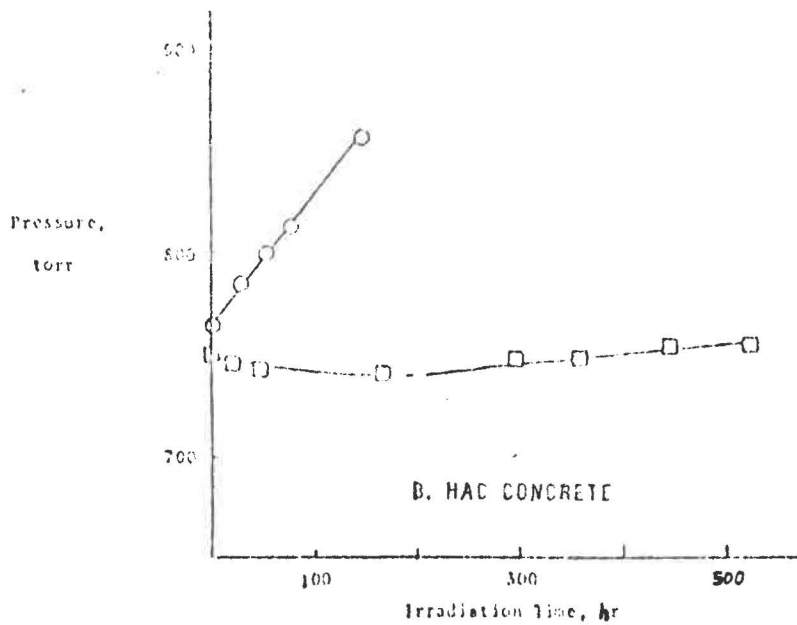


FIGURE 4
EFFECT OF WATER IN CONCRETE
ON RADIOLYTIC GAS GENERATION



As with other types of concrete, hydrogen gas is produced by radiolysis of the residual water in the pellets. But, because of the lower water content (than that in poured concrete), the $G(H_2)$ values were lower. Three compositions of portland type I cement, $^{238}\text{PuO}_2$, and 65 weight percent of simulated ash (SRL ash, Mound Lab ash, bone char) were analyzed for hydrogen production. The measured results are presented in Table 5. The $G(H_2)$ values ranged from 0.003-0.009, among the lowest concrete values tested. These lower values reduce the significance of radiolytic gas production from concrete when considering it as an immobilizing agent for TRU waste.

Related modified concrete matrix waste form development studies are being conducted at the Oak Ridge National Laboratory. The ORNL FUETAP concrete (33), formed under elevated temperature and pressure, is being tested to incorporate up to 15 weight percent of radioactive sludge. A determination of the radiolytic gas generation characteristics of FUETAP concrete specimens containing actual radioactive waste sludge is planned (33). An examination of the recombination rate of hydrogen and oxygen in the presence of concrete and/or other solids having possible catalytic properties is in progress. Oxygen is a product of alpha radiolysis when high specific activity sludge is incorporated into concrete (4).

The gamma radiolysis of concrete containing fission product sludges has also been studied at SRL (4,28). With gamma radiolysis, hydrogen is the only significant product. Hydrogen reaches a steady state pressure that increases with increasing radiation intensities. Equilibrium H_2 pressures, at realistic dose rates, varied from 8-28 psi. When nitrate and nitrite ions were present, gamma radiolysis also produced oxygen and nitrous oxide.

The observed failure to reach a steady state pressure (at least up to 200 psi) reveals (28) a difference in mechanism between alpha and gamma radiolysis. This results from a difference in the spatial distribution of the H and OH radicals formed by the two types of radiation. Alpha particles lose energy in a much smaller volume than gamma rays, thus the reaction intermediates are formed much closer together.

2.6.3 Total Gas Generation and Pressurization:

The rate of gas generation from TRU ash encapsulated in concrete can be calculated after several assumptions are made. These are: The concrete-TRU ash mix is contained in 210 liter drums 90 percent full; the density of the waste matrix is 1.6 kg/l (16,21); the waste contains 200g of ^{238}Pu --the maximum concentration limit (1), and all alpha decay energy is absorbed by the waste matrix. The resultant waste matrix weighs 300 kg, and contains approximately 91 kg of water, assuming that the concrete is poured and has 30 weight percent of water. The measured $G(\text{total gas})$ values for non-heated concrete-TRU ash (for HAC and Portland type I cement) range from about 0.03-0.6. The resultant calculated total gas generation rate range is:

for 200g ^{238}Pu , 0.046-0.93 moles/year/drum (non-heated)

TABLE 5

PRESSED CONCRETE PELLET RESULTS

Simulated Waste:	G(H ₂)
SRL Ash (primarily Ca, Ti)	0.005
ML Ash (primarily Si, Ca)	0.009
Bone Char* (primarily Ca, C)	0.003

pellet weight composition:

65 percent ash (dry), 35 percent portland type I cement (dry),
3 percent water

*commercial absorbent, used to sorb Pu

For concrete-TRU ash heated to 100° or 200°C, or for pressed pellets, G(H₂) values have been measured in the range of 0.0003 to 0.031. Similarly, G(total gas) values ranges from 0.023 down to non-detectability (assumed greater than zero; 0.0003 for calculational purposes). The resultant calculated total gas generation rate range is:

for 200g ²³⁹Pu, 0.0005-0.035 moles/year/drum (heated)

The long-term pressure increase due to hydrogen accumulation inside a 210 liter drum, as a function of storage time, is illustrated in Figure 5. G(H₂) values range from 0.005 up to 0.3, representative of various waste treatments, as indicated; 200g of pure ²³⁹Pu was assumed for calculations. The void volume inside the drum is 21 liters plus another 21 liters due to an assumed 10 percent porosity for the concrete; total void volume equals 42 liters. This void volume could be equated to an equivalent volume of gas accumulation in a geologic repository; drums will not hold a pressure much greater than one atmosphere (3). Curvature in the lines is due to radioactive decay of the ²³⁹Pu. The dashed portion of the lines was calculated by assuming that the gas generation rate is invariant during the long storage times. There are factors which could cause the G(H₂) values to decrease. For example, as the hydrogen pressure increases, hydrogen could become involved in radiolytic back reactions. Tests at SRL have shown that this does not occur up to the H₂ pressures of 160 psi (28). Higher pressures are now being tested. Another factor that could cause G(H₂) to decrease is the loss of the water in the concrete due to radiolysis yielding hydrogen. This will not be a factor for the cases illustrated in Figure 5 for more than 10⁴ years.

2.7 Assorted Radiolysis Observations

Based on the data of Zerwekh (3), the radiolytic degradation of cellulose and polyethylene (low density) contributes significantly more gas generation than that of rubbers (decreasing degradation order of): isoprene (surgeons gloves), Hypalon (drybox gloves), and neoprene (drybox gloves).

The high-density, 100 percent cross linked polyethylene used to line (2.4 mm, 100 mil) TRU waste barrels shows a remarkable resistance to radiolytic attack (3).

The largest G(gas) value yet measured (14), 8-11, is for polyvinyl chloride (PVC). The G value for PVC also appears to be increasing with increasing dose rate (34). Salovey (35) stated that the G value for PVC is 23. Studies are continuing.

Studies at LASL (2,3) have compared the radiolytic degradation of dry cellulose versus wet cellulose. The wet cellulose were found to degrade at approximately the same rate, and occasionally faster than the dry; this should be due to the additional degradation of sorbed water. The Rocky Flats studies (6) are in disagreement with that result, reporting a G(gas) value for the wet matrix one-half that of the dry matrix.

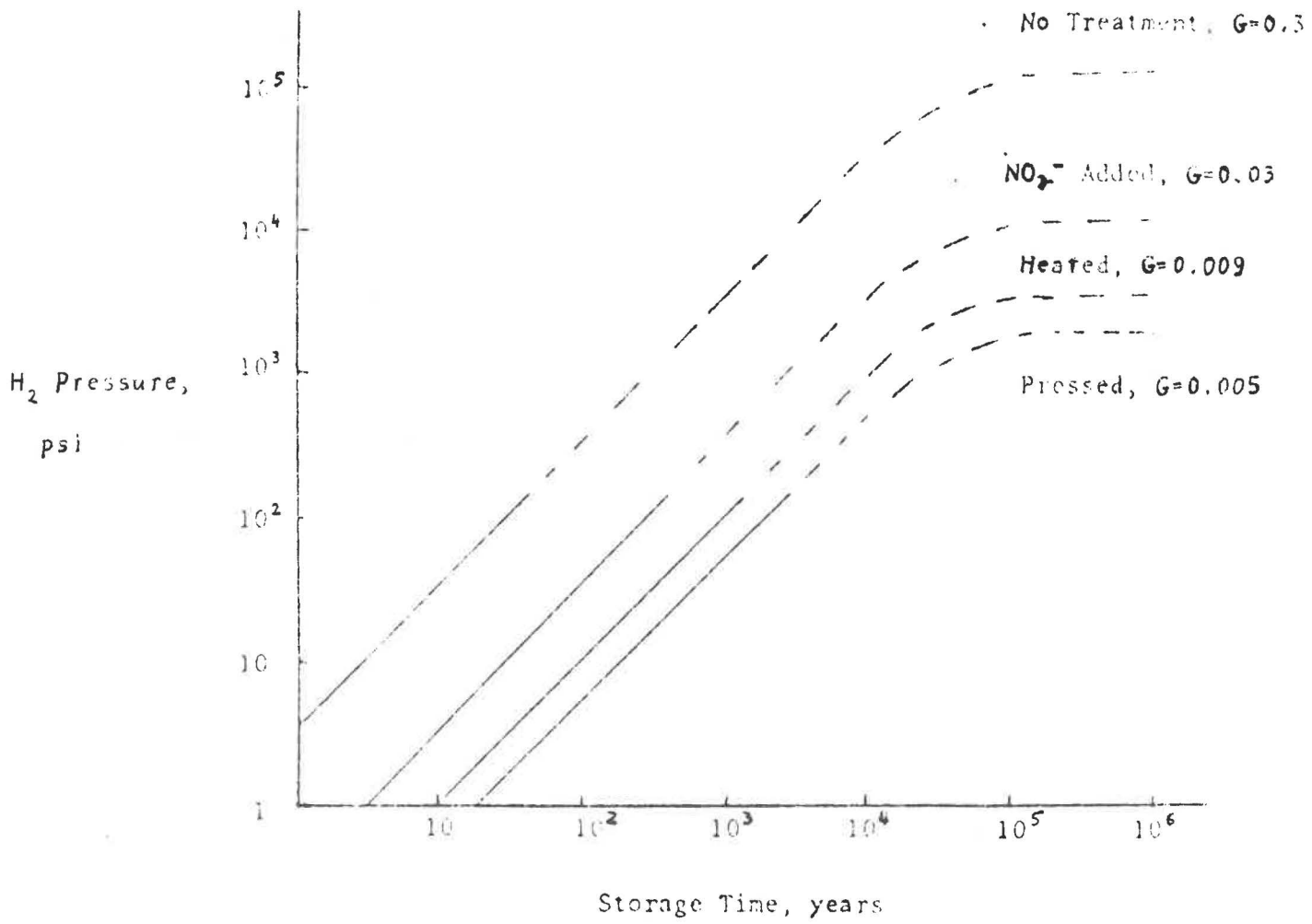


FIGURE 5
 CONCRETE-TRU ASH MATRIX
 LONG-TERM PRESSURE INCREASE/DRUM

The alpha radiolysis of asphalts, used for low- and intermediate-level waste encapsulation in Europe (36), was reported (37); ^{210}Po was used as the alpha contaminant. Using these data, Kosiewicz (14) calculated a G(gas) value of about 0.2; initial lab studies at LASL (14) indicate a G(gas) for asphalt of about 0.5-1.0.

The radiolytic degradation of first stage process sludges has not been measured experimentally, but can be calculated by the radiolysis of its 70 weight percent water content. For an average dose rate of 6.9 alpha Ci/drum (13), and an estimated G(gas) of 1.0 (21), sludge radiolysis yields 0.7 moles of gas/year/drum. This radiolytic gas generation rate is significantly higher than that of any other existing TRU waste matrix; this may cast some doubt on the acceptability of such sludges for terminal isolation.

The effects of alpha and gamma radiolysis on glass radioactive waste forms has been evaluated (38,39,40,41) and found not to produce gaseous products.

In existing TRU wastes contaminated with plutonium nitrate, the contaminant was observed (3) to change to plutonium oxide in approximately one month when exposed to an air atmosphere.

After termination of cellulosic radiolysis tests, Zerwekh (3) observed a tan powder, containing approximately 50 percent of the original contaminant, at the bottom of the test cylinders. This tan powder has a very low density, is highly contaminated, and is easily airborne. The existence of this particulate would probably necessitate careful handling if existing, high-contaminated, temporarily-stored TRU wastes are reprocessed.

If waste in storage is to be reprocessed, the oldest waste is potentially the most hazardous because it is the most degraded and not well categorized (3).

3.0 THERMAL DEGRADATION DATA

The thermal degradation of organic matrix TRU waste materials is currently under measurement at LASL (2,14,17,42,43,44). Waste matrices under study include: paper, cotton, and composite, plus polyethylene. Temperatures of interest are 20^o, 40^o, 70^o, and 100^oC. The 40^o temperature is probably of most interest for the WIPP TRU waste repository once filled and sealed. Thermal degradation was monitored to determine gas generation rates and also to determine threshold decomposition temperatures.

3.1 Threshold Decomposition Temperatures

Preliminary thermal degradation studies at LASL (17,42), utilizing thermal gravimetric analysis, determined threshold decomposition temperatures in air ranging from 175^o to 205^oC for cellulose, 150^o to 210^oC for plastics (excluding Teflon), and 165^o to 195^oC for rubber materials commonly found in laboratory waste. A study at the Battelle Pacific Northwest Laboratory (45) determined the endothermic starting point (pyrolysis, in nitrogen, utilizing differential thermal analysis) for similar waste matrix materials. At ORNL (46), a study on the spontaneous combustion, oxidation, and pyrolysis of combustible solid wastes (cellulose, polyethylene, plywood, etc.) contaminated with TRU elements was also made. Polyethylene (low-density) had the lowest decomposition (melting) temperature (17,42) of 80^oC. Godbee at ORNL (46), reported a melting/softening range for polyethylene of 91-132^oC, and a similar range of 102-126^oC for a mixture of 75 weight percent of cellulose plus 25 weight percent polyethylene.

Almost all other materials had threshold decomposition points (17,42) at temperatures greater than 250^oC. These results (45) confirm earlier work done at LASL (47) where rags, paper, polyethylene, PVC, latex, butasol, and neosol did not begin to decompose (in air) up to 150^oC, although both polyethylene and PVC began to soften. At 200^oC, all test specimens began to char and decompose. Asphalt (bitumen) began to decompose at 275^oC (34).

Considering that oxygen in TRU-contaminated waste drums would be consumed by radiolysis (14,22), LASL (42) repeated threshold decomposition studies (using TGA) in an anaerobic (nitrogen) atmosphere for cellulose, polyethylene, asphalt, lucite, and hypalon rubber. Investigations were also conducted on the potential effects (on threshold decomposition temperatures) of catalysts which could be found or formed by storing drums of TRU waste in a salt mine repository. Catalysts included: none, NaCl, Fe₂O₃, FeCl₂, and Fe powder, with loadings ranging from 2 to 38 weight percent. The data for threshold decomposition temperatures, in both air and nitrogen (14) are listed in Table 6. The effect of the catalysts was relatively minor, changing threshold decomposition temperatures no more than plus/minus 30^oC. All of the measured decomposition temperatures are significantly higher than would be credible for the TRU waste horizon of the WIPP.

3.2 Thermal Decomposition, Gas Generation

No gas generation from the degradation of organic matrices at temperatures of 100^oC and below has been observed previously, due primarily to limited

TABLE 6

THRESHOLD DECOMPOSITION TEMPERATURES OF ORGANIC WASTE MATRICES
(°C)

Material:	<u>In Air:</u>	<u>In Nitrogen, With Indicated Catalyst:</u>				
		None	NaCl	Fe ₂ O ₃	FeCl ₂	Fe
Cellulosics	185-195	185	180	185	170-195	195
Cotton	185-190	185	195	200	170-195	205
Wood	175	---	---	---	---	---
Polyethylene	210	320	290	295	330	335
PVC Gloves	150	---	---	---	---	---
Lucite	170-175	150	155	170	185	160
Teflon	430-435	---	---	---	---	---
Hypalon	165	160	175	160	155	160
Neoprene	175-180	---	---	---	---	---
Asphalt	275	290	---	---	---	---

detection techniques. Observation of accumulated gases via pressurization is a much more sensitive indication of thermal waste degradation than is weight loss via thermal gravimetric analysis (TGA). It is the technique used at LASL (14) to measure both degradation and gas generation rates. These thermal gas generation experiments are essentially long-term (years) surveillance studies (14) because of low degradation rates.

Tentative gas generation rates (14) for cellulose, polyethylene, and organic composite are listed in Table 7. Some gas generation has been observed at 100°C and 70°C, but not yet at 40°C. Although the measured rates have been converted into units of moles of gas/year/drum of waste (51.4 kg), extreme caution should be used in interpretation of such data. Sparsities or inconsistencies of measured data (14) make it very difficult to discern significant, quantitative trends. The oxygen (air) present in the test cylinders becomes depleted initially, creating a partial vacuum which must be offset by generation of degradation product gases (14). Although test cylinders were monitored for up to 436 days and are continuing to be monitored, the data presented must still be considered experimentally uncertain. The possibility also exists that bacterial degradation may be evolving some gas, thereby masking trends from thermally generated gases. This bacterial gas generation will be discussed in Section 4.0.

Qualitatively, more gas is generated at 100°C than at 70°C. Experiments combining radiolysis and thermal degradation at LASL (14) have yielded data substantiating this; tentative data is listed elsewhere (14).

Murphy (48) stated that cellulose decomposes even at room temperature at a very slow but finite rate. He proposed the following equation for calculating the cellulose gas generation rate:

$$\text{Log}_{10} Q = 16.3 - 7.4 \times 10^3/T \text{ } ^\circ\text{K}$$

where Q is the gas generation rate in cm³ (STP)/year/g.

The LASL-measured rate of gas generation for paper at 70°C is about five orders of magnitude greater than that predicted by Murphy's relationship. Still, no one had detected gas generation from thermal degradation at temperatures of 100°C or less-- not until the current LASL results (2,14,43,44) were presented.

Using Murphy's equation above, the calculated gas generation rate at 40°C should be about a factor of 100 less than that at 70°C. Based on LASL measured rates at 70°C for cellulose and polyethylene, this relationship yields an approximate gas generation rate of about 0.02 moles/yr/drum (51.4 kg of waste matrix). Utilizing a simplistic chemistry relationship, namely that reaction rates double for every 10°C rise in temperature, the gas generation rates at 40°C for the organic waste matrices studied can be estimated/extrapolated at approximately 0.2 moles/yr/drum. The gas generation rate at 40°C is, consequently, bounded by 0.02 and 0.2 moles/year/ drum by the two methods of calculation. Murphy (48) also postulated that thermal decomposition of cellulose should decrease exponentially as a function of time. He did not provide a relationship; assume $Q = C_1 \exp(-C_2 t)$. No kinetic data are yet available for the temperature range of primary interest, 40° to 70°C, to estimate how much the gas generation rates will decrease, for example, in 100 years.

The LASL-analyzed compositions of gases (2) generated by thermal degradation are presented in Table 8.

In order to evaluate the effectiveness of catalysts on gas generation by thermal degradation, Kosiewicz (34) doped paper and polyethylene separately with NaCl or FeCl₂, at 2 weight percent loading, in air at 40°C. After 8 months of observation, the following tentative conclusions were reached (34):

1. NaCl may catalyze the decomposition of polyethylene and, to a smaller extent, that of paper, at 40°C.
2. FeCl₂ appears to catalyze the decomposition of paper at 40°C.
3. Some very slight decomposition (thermal or bacterial) appears to be occurring in the absence of catalysts or Pu contamination at 40°C.

3.3 Thermal Dewatering

Other interesting data gathered from the thermal studies include:

1. When cellulosic wastes at LASL were heated through the range of 40-110°C, 2 to 3 weight percent of sorbed water was evolved (14). This range could possibly change significantly if the waste matrix was stored in a more humid environment than that which exists at Los Alamos.
2. Dewatering of LASL process sludges was determined (44) at 25°, 40°, 70°, and 100°C as a function of time. These sludges are primarily ferric hydroxide precipitants containing about 30 percent solids. Experimental conditions included flowing dry nitrogen over gram size samples of sludge contained in a thermobalance. This arrangement should be somewhat representative of a breached waste drum in a salt repository, with the salt acting as a desiccant for released water vapor. Times for 100 percent dewatering of the sludge samples ranged from 1 hour at 100° to 35 hours at 25°C. In summary, drums containing sludge waste could be expected to release essentially all their water in a very short (geological) time due simply to attainment of equilibrium water vapor pressure.
3. Cement paste has been used at LASL (2) for immobilization of certain waste materials. Currently, it comprises the second-ranked contributor (by volume) to the LASL waste inventory. Rates of thermal dewatering of cement paste at 40°C and 100°C were performed for comparison with the process sludge material. The cement paste samples utilized (dating from 1974) contained no lower than 10 weight percent water (as determined by heating to 400°C) and may be considered more nearly similar to concrete than to "cement paste." From preliminary data, it appears that cement paste-concrete is much more difficult to dewater than process sludge. Cement paste-concrete may not dewater completely at a credible boundary temperature of 70°C in the WIPP TRU waste horizon.

TABLE 7

TENTATIVE GAS GENERATION RATES FROM THERMAL DEGRADATION

(Average drum = 51.4 kg of waste matrix)

<u>Matrix:</u>	<u>Gas Generation Rate (moles/year/drum)</u>		
	100°C	70°C	40°C
Paper	--	1.3	*
Composite	44	--	*
Polyethylene	--	1.9	*
Cotton	--	5.2	*

*estimated at 0.02-0.2 mole/year/drum

TABLE 8

APPROXIMATE GAS COMPOSITIONS FROM THERMAL DEGRADATION AT 70°C

	(mole percent)				
	CO ₂	CO	H ₂	O ₂	CH ₄
Paper	80%	19%	--	1%	--
Cotton	31%	11%	(1%)	58%	--
Composite (100°C)	76%	3%	14%	7%	(1%)
Polyethylene	3%	1%	3%	93%	--

The potential impacts of thermally volatilized water could include:

1. Dissolution of salt to yield brine pools or lenses.
2. High humidity in mine, pumped out via ventilation system during working phase of facility.
3. Potential enhanced corrosion of metallic waste canisters, instrumentation, and mining-engineering equipment.
4. Hydrolysis, hydration of minerals (anhydrite, clays, etc.) with consequent potential swelling effects.
5. Leaching or dissolution of waste materials resulting in the potential water/brine mobilization of radionuclides as true solutions, colloidal solutions, or as entrained particulate material.

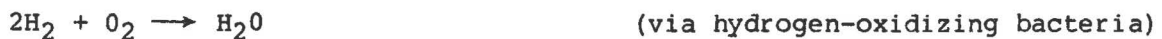
4.0 BACTERIAL DEGRADATION DATA

Transuranic-contaminated wastes can serve as the energy source for microbial growth. Heterotrophic bacteria or fungi can utilize the organic content of organic matrix TRU wastes as nutrients. Lithotrophic microbes can synthesize organic matter for their needs from inorganic substances found in the waste container or near-field environment, e.g., oxidizable substances such as H_2 , NH_4^+ , SO_3^{2-} , Fe^{2+} , or H_2S .

Existing organic, unprocessed TRU wastes could contain adequate quantities and varieties of bacteria and fungi to cause significant biological degradation. These microbes originate from environmental and human sources in the laboratory and in soil that is used to cover the waste containers in temporary, retrievable storage. The presence or distribution of such microbes is quite widespread. For example, in a WIPP-funded microbial chelate degradation study (8), measured degradation rates were nearly identical for two separate experiments where a microbial soil inoculum was utilized in one case and not in the other. This indicates that sufficient microbes were already present on the organic waste substrate utilized. There will be, of course, a large variability in the type and quantity of microbes present, as a function of waste composition, environmental conditions, and trace contaminants.

Microbial growth in, or degradation of organic matrix TRU waste can lead to several consequences including significant gas generation. A WIPP laboratory and field study of microbial waste degradation concerns has been in progress since May, 1978. These studies are conducted by the University of New Mexico biology department, with laboratory and field support from the Los Alamos Scientific Laboratory, H-9 division, and consulting assistance by C. E. ZoBell, Scripps Institution of Oceanography. Overall objectives of the total microbial degradation program are summarized elsewhere (49,50); descriptions of individual studies and recent progress are found elsewhere (8,50,51,52).

The production, consumption, and transformation of gases by microorganisms have been studied extensively; a recent review was made by Cole (53). Gases can be produced by bacterial decomposition by the metabolic processes of anaerobic or aerobic respiration, fermentation, denitrification, sulfate reduction, methanogenesis, etc. Examples of microbial consumption of gases produced abiotically (primarily H_2) are as follows:



An example of microbial transformation of gases is the anaerobic reaction:



A major effort has been made to quantify the rate and composition of gases produced from microbial action on organic matrix wastes under a variety of conditions. All available applicable data are presented. There is no question that CO_2 will be produced regardless of the conditions present (50).

4.1 Experimental

The organic waste matrices investigated in this study include: (1) LASL organic composite waste (approximately 35 percent cellulose, 23 percent polyethylene, 12 percent polyvinylchloride, 15 percent neoprene, and 15 percent Hypalon rubber), (2) sawdust, (3) asphalt, (4) organic composite minus the cellulosic component, and (5) carboxymethyl cellulose. The sawdust is representative of plywood used in fiberglass reinforced polyester plywood boxes (DOT 7A) currently used for TRU waste disposal. Plywood consists primarily of cellulose, with some lignin which degrades much more slowly (50). Carboxymethyl cellulose (activated cellulose) is frequently used in microbiological media to detect cellulose degrading bacteria (50). The asphalt used represents that used in the low-level waste volume reduction (bitumenization) system (54) of the Werner and Pfleiderer Corporation. This system is routinely used in Europe (36). The asphalt was manufactured and supplied by the Industrial Fuel and Asphalt Company of Indiana, Inc.

The variables utilized in the experimental studies, other than waste matrix, include:

- (a) Incubation Temperature (25°, 40°, 50°, 60°, and 70°C),
- (b) Atmosphere (aerobic and anaerobic),
- (c) Solution content - deionized water, WIPP brine "B" (predominately NaCl), phosphate buffer (pH 7.0, 0.01M PO₄), and bacterial nutrient solution.
- (d) Solution/waste ratio - "saturated," made by adding 10 ml of solution ("91 percent H₂O," brine, or nutrient) to 1 g of waste matrix; "1 percent water," made by adding 10 microliters of water to 1 g of waste, to insure that a minimum amount of water was present, necessary for microbial activity (49). This much moisture is probably present in the waste due to sorbed water or ambient humidity; and, "wet," used in preliminary experiments, made by adding 1 ml of phosphate buffer to 1 g of waste.
- (e) Microbial Inoculant - 20 mg of soil inoculant added to 1 g of waste matrix in preliminary experiments, an equivalent amount added as a portion of the liquid in the most recent studies.

Control samples, sterilized with steam, were utilized for background subtraction.

Gas produced by microbial action was initially analyzed using an automated gas chromatograph with a thermal conductivity detector. Detection sensitivity for the potential gases of interest, CO₂, CH₄, CO, H₂S, H₂, SO₂, etc., is 6 x 10⁻¹⁰ g/sec; minimum detectable level for CO₂ is 2 x 10⁻⁸ moles/100 microliter sample. The only significant gas detected (8) as a degradation product of LASL composite waste was CO₂. The gas chromatograph analysis was replaced by a more precise routine analysis for CO₂

alone. This analysis consists of the titration of CO₂ trapped in an absorbent 0.1M barium hydroxide solution. Supplemental gas chromatograph analyses, at three month intervals, will be used for the detection of other gases.

4.2 Gas Generation Results and Discussion

The preliminary gas generation data, measured over a 90-day incubation period, are summarized in Table 9. Data for LASL organic composite waste and carboxymethyl-cellulose (CM-cellulose), as a function of temperature, are presented both under aerobic and anaerobic conditions. All samples consisted of 1 g of waste plus 1 ml of phosphate buffer, a "wet" system. The data values are in terms of moles of CO₂ generated per year per drum of waste.

It has been assumed that the cellulosic component of the composite waste is the substrate predominantly used for microbial CO₂ evolution. For comparative purposes, the CM-cellulose data have been presented for an 18 kg quantity, equivalent to the cellulosic content in the composite (35 percent of 51.4 kg = 18 kg). The correspondence is not very good. (It is significantly better for the sawdust data--to be presented later). However, other components in the composite can serve as a microbial nutrient source of nitrogen and phosphorus. These may yield further cellulose degradation and gas generation from the composite as compared to that from the CM-cellulose. To check the biodegradability of other components in the composite matrix, a test system of composite minus the 35 percent cellulose was incubated for approximately 100 days. Preliminary analysis indicated no appreciable CO₂ generation (greater than or equal to zero). It is possible that the rubber component of the composite mix will degrade very slowly, yielding gas; it is not likely that the polyethylene will be microbially attacked.

No evolution of methane was observed, although it was initially expected. This was probably due to the lack of an adequate methanogenic inoculum and/or a lack of strict anaerobic conditions. The appropriate condition for methanogenesis will be met in experimental studies planned for FY80. However, methane could be a major product if or when the WIPP TRU waste horizon becomes anaerobic (8). Methane would be substituted for CO₂ gas on a near mole-for-mole basis (55), and would be generated at a slower rate than that of CO₂.

Data from a related study (56) of microbial decomposition of the cellulosic component of various common papers and cloths are shown in Table 10. The rates presented (56) are indicative of microbial degradation under optimized anaerobic (-250mV) conditions. Vitamins and salts were added to stimulate microbial activity. The gas produced was 56-59 percent methane, the remainder was primarily CO₂. Data from similar studies (56,57,58) of anaerobic decomposition of tissue paper indicated that 1.6 moles of methane per mole of cellulose (glucose) could be produced per week.

TABLE 9

PRELIMINARY GAS GENERATION RATES FROM BACTERIAL DEGRADATION

MATRIX:	(moles CO ₂ /year/drum)		
	T ^o C	AEROBIC	ANAEROBIC
LASL Composite (51.4 kg)	25 ^o	0.9	1.2
	40 ^o	7.6	1.7
	50 ^o	12.3	32.2
	60 ^o	12.3	3.8
	70 ^o	0.1	0.1
CM-Cellulose (18 kg)	25 ^o	3.2	0.006
	40 ^o	2.4	2.9
	50 ^o	6.4	0.9
	60 ^o	1.4	1.4
	70 ^o	0.2	0.2

TABLE 10

DEGRADATION OF CELLULOSICS UNDER OPTIMUM ANAEROBIC CONDITIONS (56)

MATERIAL:	CELLULOSE CONTENT (% Dry Weight)	DEGRADATION RATE (% Cellulose Degraded per Week)
Bookprint	54	11.2
Brown Paper Bags	65	18.7
Cardboard Boxes	66	20.0
Cardboard, Corrugated	61	19.2
Cheesecloth	93	19.0
Computer Paper	74	22.5
Cotton Batting	96	18.5
Filter Paper	90	24.2
Newsprint	56	10.5
Paper Towels	69	21.5
Tissue, Kleenex	76	24.0
Toilet Paper	71	23.0
Writing Paper	76	23.2

Degradation rates of contaminated organic matrix wastes are lower than the optimized rates (56) reported in Table 10. This is due to the unfavorable conditions (e.g., lack of vitamin/nutrient supplements, potential high salt concentrations, chemical and/or radioactive contaminants, etc.) anticipated for wastes stored in a bedded salt geologic isolation environment--and also as used in WIPP-specific test simulations.

Figure 6 illustrates the temperature dependence of CO₂ gas generation from the bacterial degradation of organic composite waste (preliminary data from Table 9). The peak in gas generation, for both the aerobic and anaerobic environments, occurs at about 50°C. Data measured in the 40°C to 60°C temperature range may be the most applicable for geologic isolation conditions, assuming heat generating wastes are also present. Microbial action occurring inside a drum may temporarily raise the drum temperature above the mine ambient temperature.

Since the preliminary data (8) in Table 9 were obtained, more waste matrices and variables have been added to the experimental system (52). Sufficient data points (3-5, but only 2 for data at 40°C) have been accumulated (52) over a period of 92-112 days to justify fitting the data by linear regression analysis. In most cases, this linear fit has been quite good, as evidenced by the high R-square (goodness of fit) values obtained. The raw data (not included) are presented as:

$$G = (\text{rate}) (\text{incubation period, days}) + \text{intercept},$$

where G is the milligrams of CO₂ accumulated per gram of waste, and the rate is expressed in mg of CO₂ generated per day per gram of waste. The intercept values account for initial values of atmospheric CO₂ present in the experimental apparatus; they may also be a function of the initial background sterilization procedure. The net amount of gas accumulated is calculated by:

$$G_{\text{net}} = G_{\text{gross}} - G_{\text{sterile background}}.$$

The gross G values determined include predominantly bacterially generated gas, but may also include any thermally produced gas. The background subtraction, however, removes this thermal component.

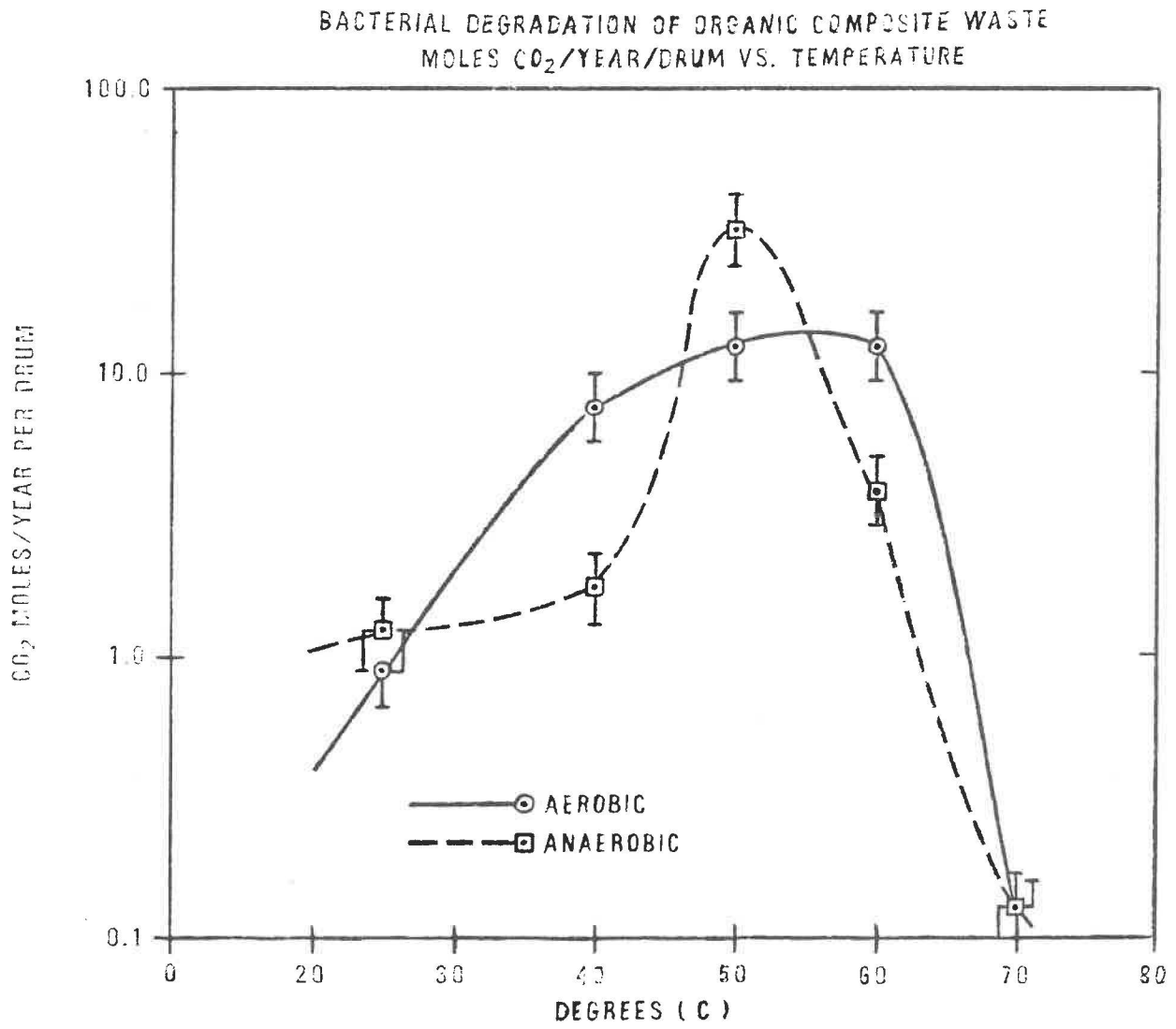
The most recent data (52) for composite waste, sawdust, and asphalt, all under a variety of conditions, are presented in Table 11, in terms of moles of CO₂ generated per year per drum of waste. To minimize any skewing of the results, for predictive purposes, caused by relatively large zero-time intercept values, the values presented were calculated as:

$$G = ((\text{rate})(100\text{years}) + \text{intercept}) / 100 \text{ years}.$$

The values can therefore be extrapolated as rates simply by multiplying by the appropriate time factor.

The accuracy of the bacterial data presented is estimated at plus/minus 25 percent. However, the confidence interval or precision of such data is very large, probably hundreds of percent. This is due to the inherent variability

FIGURE 6



of bacterial systems, the quantity and type of bacteria present, non-homogeneity of waste matrices, and trace contaminants present. Individual series of tests can be accurately compared for magnitudes and trends, but comparisons of several series of tests must be done with some latitude.

The data in Table 11 are presented for waste packages containing different representative amounts of waste. The 51.4 kg of composite waste in a 210-liter drum has been explained previously. For sawdust, a plywood simulant in this case, 153 kg corresponds to the calculated weight (59) of plywood (0.75 inch thick) in a 4ftx4ftx7ft DOT 7A FRP plywood box currently used for TRU waste storage. Since this sawdust-plywood consists predominantly of cellulose, the values are recalculated and presented for 18 kg, for comparison with the data for the organic composite waste which also contains 18 kg of cellulose. For asphalt, the 135 kg value originates with the average amount of asphalt (bitumen) used in the low-level waste solidification process at the Eurochemic Facility in Mol, Belgium (36). In this case, each 210-liter drum contains about 180 liters of solidified waste weighing 245 kg; of this weight, 55 percent, or 135 kg, is bitumen, the rest is waste solids.

For the LASL composite waste, the data presented in Table 11 generally overlap or are in agreement with the preliminary data presented in Table 9 for both the 51.4 kg of composite and the 18 kg of CM-cellulose. The preliminary data (8) are for a wet waste system containing 1 ml of buffer solution to 1 g of waste rather than the saturated or dry (1 percent water) conditions of the newer (52) results.

The current composite results tend to indicate that slightly more gas is generated under anaerobic conditions than under an aerobic atmosphere for most of the system solution variables. An anaerobic environment is more probable for a TRU waste repository over long periods of time. Less gas appears to be generated when the waste is relatively dry, with 1 percent water added, than when the system is saturated or inundated with water. The presence of brine, rather than water, does not appear to have an overall significant effect on rates of gas generation. Temperature effects or trends on gas generation do not appear to be as clear cut as they were on the preliminary series of tests (Table 9), but this may be due to differences in water/waste ratios.

With the sawdust-plywood test system, a gas generation temperature dependence is again not evident. What is evident, however, is that a plywood box has the potential to produce large quantities of CO₂ gas under most of the conditions investigated. A primary reason for this is because of the large mass of the box and its high cellulosic content. In dirt-covered temporary-storage environs, a FRP plywood box containing TRU wastes has a great potential for being contaminated with appropriate bacteria. The plywood is, however, shielded somewhat from the bacteria by a thick (approximately one-quarter-inch thick) layer of fiberglass reinforced polyester resin on the outside and possibly a polyethylene liner or bags on the inside. Although the polyester resin was not specifically tested here, it is susceptible to bacterial degradation, presumably at a slower rate than cellulose. Also, solid plywood should degrade at a slower rate than that of finely ground sawdust with a high surface area.

TABLE 11

NET BACTERIAL CO₂ GAS GENERATION FOR VARIOUS ENVIRONMENTS

Environment	(Moles/Year/Container)					
	25°C	40°C	70°C	25°C	40°C	70°C
	AEROBIC			ANAEROBIC		
	<u>LASL Composite (51.4 kg/drum)</u>					
Water, Sat.:	1.6	1.8	3.1	4.2	0.6	3.4
Brine :	(0)	5.2	5.5	1.2	7.8	(0)
Nutrient :	3.1	1.5	(0)	3.6	1.4	7.3
Water, 1% :	(0)	1.3	4.2	0.3	2.6	2.5
	<u>Sawdust-Plywood (153 kg box)</u>					
Water, Sat.:	14.3	10.3	14.0	26.2	4.7	23.0
Brine :	(0)	11.6	18.6	11.8	(25)	6.8
Nutrient :	13.5	2.8	18.0	12.2	6.9	12.6
Water, 1% :	3.0	9.7	2.8	11.3	17.3	17.3
	<u>Sawdust-Plywood (18 kg)</u>					
Water, Sat.:	1.7	1.2	1.7	3.1	0.6	2.7
Brine :	(0)	1.4	2.2	1.4	(3)	0.8
Nutrient :	1.6	0.3	2.1	1.4	0.8	1.5
Water, 1% :	0.4	1.1	0.3	1.3	2.0	2.0
	<u>Asphalt (135 kg/drum)</u>					
Water, Sat.:	2.1	(0)	(0)	0.6	1.9	1.9
Brine :	2.6	(0)	8.4	(0)	0.9	1.6
Nutrient :	3.7	1.0	0.9	4.3	0.3	(0)
Water, 1% :	0.01	0.9	0.03	4.8	0.9	(0)

July, 1979

When the sawdust-plywood values for an 18 kg mass are compared with the organic composite results, a fairly good agreement is reached, further verifying the assumption of composite gas generation being due primarily from its cellulosic content. Other observations for the sawdust-plywood system are basically the same as those made for the composite.

Gas generation from bacterial degradation of asphalt appears to be comparable in magnitude to the composite results at 25°C for both aerobic and anaerobic environments. Gas generation is greater for anaerobic conditions with a dry (1 percent water) waste system compared to aerobic conditions, but apparently opposite for saturated water and brine systems. Again, monolithic drums of asphalt would undoubtedly degrade slower than the results presented here obtained by testing small, but higher surface area to volume samples.

Microbial gas generation studies are still in progress; the data presented here should not be taken as final. Longer-term data should help clarify the trends and tentative conclusions. One thing is quite obvious, however-- Bacterial degradation of organic waste matrices has the potential to produce larger quantities of gas than any other degradation mechanism studied. This potential requires the presence of adequate types and quantities of bacteria in or on waste packages, with such contamination occurring either before or after package sealing. This is a relatively safe assumption to make. It should also be assumed that any kind of microorganism may find its way into the repository during excavation and emplacement operations. Some fraction of these microorganisms may survive and adapt to the existing environment, potentially resulting in significant waste degradation (49).

5.0 CHEMICAL CORROSION DATA

The generation of hydrogen gas from the corrosion of the mild steel alloy used in TRU waste containers, 210 liter (55 gallon) drums, is the only long-term chemical degradation mechanism of significance yielding gaseous reaction products.

Braithwaite (60) measured the rate of corrosion of 1018 mild steel in inundated saturated NaCl brine at 25°C by measuring the quantity of hydrogen produced or oxygen consumed. These corrosion rates and gaseous quantities are shown in Table 12. The most sensitive technique for measuring these corrosion rates, as used in the most recent studies at Sandia (61), is to measure the gases produced or consumed with a system coupled mass spectrometer.

In order to better quantify gas consumption or generation rates due to steel corrosion under more probable, non-inundated repository environments, another series of corrosion tests was conducted. The results of the initial phase (after six months) of these corrosion tests (61) are also shown in Table 12. Test cells were originally filled with air to produce a realistic initial repository storage environment. The amount of hydrogen gas produced in all six environments was negligible as would be expected (61) when oxygen is still present. Once the oxygen is consumed, as is presently the case with the 100 percent relative humidity plus crushed salt test, then hydrogen gas will be produced via the cathodic reduction of water.

Surveying the non-inundated corrosion data, the most significant result is the reduction in oxygen consumption/corrosion rates compared to those produced under inundated conditions; the rates are typically an order of magnitude or more slower. A further analysis of these corrosion data, as applied to expected waste container lifetime, is made elsewhere (11).

For corrosion under conditions of geologic isolation, the following generalizations can be made regarding gas generation or consumption:

1. Any oxygen present will substantially reduce the amount of hydrogen produced.
2. Under aerated conditions, corrosion reactions will result in a net decrease in total number of moles of gas present due to oxygen consumption.
3. Overall, if the oxygen is depleted and water is present, a total of 672 moles of H₂ can theoretically be produced from the complete corrosion of a 210 l drum, at a maximum rate (at 25°C) of 2 moles/year. A 210 l drum has a total surface area of 4 m².
4. No hydrogen will be produced if moisture does not contact the steel drum (dry salt); the only reaction, which will be extremely slow, is:

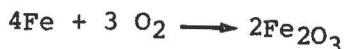


TABLE 12

MILD STEEL CORROSION AND GAS CONSUMPTION/GENERATION

(25°C)

<u>Environment</u>	<u>Rate of O₂ Consumption</u> (moles/m ² -year)	<u>Original O₂ Mole % Consumed</u>	<u>1018 Steel Corrosion Rate</u> (mm/year)
Brine, Inundated (aerated)	5.4	-	0.05
Brine, Inundated (deaerated)	0.5 H ₂ <u>produced</u>	-	0.003
32% RH*	0.3	36	0.003
75% RH	(0.09)	(11)	(0.0009)
100% RH	0.5	74	0.004
100% RH + Crushed Salt	0.6	99	0.005
Crushed Salt +1/2% Water	0.2	28	0.002
Dry Salt	0.0	0	0.0

*RH = relative humidity
(data in parentheses are being remeasured)

6.0 SUMMARY OF RESULTS

A comprehensive review and interpretation of all applicable TRU waste matrix degradation-gas generation data has been completed.

The waste matrices primarily considered in this study include:

- CELLULOSICS (paper, wood, cotton)
- PLASTICS (polyethylene, polyvinyl chloride)
- RUBBERS (neoprene, Hypalon)
- ORGANIC COMPOSITE (35 wt percent mixed cellulosics, 23 percent polyethylene, 12 percent PVC, 15 percent neoprene, and 15 percent Hypalon)
- PROCESS SLUDGES (inorganic oxides plus 60-70 wt percent water)
- CONCRETE-TRU ASH (developmental waste form)
- MILD STEEL (waste container or scrap metal)
- ASPHALT (European low-level waste encapsulant)

The first four categories of organic matrices listed above weigh, on the average, 51.4 kg and are contained in a 210 liter mild steel drum, with a high-density polyethylene liner. They are contaminated, on the average, with 0.5 grams of weapons grade plutonium, or 0.039 curies of alpha emitters. Characteristics of all waste types studied are listed in Table 2. These values are based on existing TRU wastes in temporary storage at INEL (13).

The waste degradation mechanisms being investigated in the Sandia-sponsored studies are:

- RADIOLYSIS
- THERMAL (decomposition and dewatering)
- BACTERIAL
- CHEMICAL CORROSION
- ALPHA DECAY (He generation)

The major gases produced from TRU waste degradation, in approximate order of abundance and significance, are:

H₂, CO₂, CO, H₂O, CH₄, O₂, NO_x, He.

RADIOLYSIS yields primarily H₂ (60 percent of total gases from cellulosics, 95 percent from polyethylene, 90 percent from PVC, and almost 100 percent from concrete-ash); the remainder is CO₂ and CO, predominantly. Water radiolytically degrades to H₂ and O₂. Oxygen becomes almost totally depleted in these systems, resulting in the formation of carbon oxides.

THERMAL degradation of cellulosics and composite yields about 80 percent CO₂, at 70°C, with a smaller amount of CO. The thermal release of water vapor (sorbed in sludges, moist cellulosics, etc.), even at ambient temperature, is also of significant consequence.

BACTERIAL degradation of organic matrices yields essentially only carbon dioxide in an aerobic atmosphere and also in an anaerobic environment. Methane is a potential major gas product in an anaerobic environment.

CORROSION yields hydrogen only in an anaerobic (anoxic), wet environment. In all other cases, it results in the consumption of any oxygen present.

ALPHA DECAY yields helium. Gas generation by this mechanism is so small compared to other modes of degradation that it will not be discussed further.

Gas generation resulting from each mechanism is specified in moles of gas/year/drum of waste. Variables that have been studied and that may affect degradation rates include: temperature, pressure, dose rate dependency, time, radiolytic/thermal synergism, and in-mine atmosphere (aerobic, anaerobic).

A comparison of initial, measured gas generation rates for various mechanisms and several matrices is presented in Table 13. These rates, the observed range of initial values, do not take into account factors which may tend to decrease rates over a period of years or more. These factors include pressure, localized matrix depletion due to radiolysis, unfavorable geochemical or gaseous environment, etc. Gas generation rates due to different mechanisms are not additive; the resultant (non-gas) degradation products from one mechanism, e.g., radiolysis or thermal, may not be optimal starting materials for another mechanism, e.g., bacterial. However, multiple modes of degradation can proceed simultaneously.

Bacterial

Organic matrices can serve as the energy source or nutrient for microbial growth and waste degradation. This mechanism has the greatest potential to generate significant quantities of gas from TRU-contaminated organic wastes or waste packaging. The potential will be realized only if a sufficient quantity and proper type of bacteria are present in or on the waste and whether they survive and multiply in their "in-can" and in-situ salt mine environment. Some bacteria will definitely be present in the existing organic TRU wastes and on the outside of the package, following temporary storage. Gas generation rates will depend on how well they flourish and may vary widely on a per-drum basis. Pertinent factors are:

- (a) increases in temperature from ambient up to 40° or 50°C generally yield increased gas production; rates generally decrease at 70°C.
- (b) insufficient data currently exist on bacterial gas generation as a function of time, for both rates and total quantities, for systems of interest.
- (c) the effect of increasing pressure on generation rates is not known.
- (d) The effects of actinide contamination and other chemical impurities on total gas generation require further investigation.

TABLE 13

OBSERVED RANGES OF INITIAL GAS GENERATION RATES

<u>Mechanism</u>	<u>Matrix</u>	<u>Total Gas Rate</u> (moles/year/container)	<u>Comments</u>
RADIOLYSIS	Cellulosics	0.0050-0.011	LASL, SRL
	Polyethylene	0.0072	LASL
	PVC	0.030-0.042	LASL
	Composite	0.0053	LASL
	Process Sludge	0.7	6.9 Ci
	Concrete-TRU Ash	0.046-0.93	poured, 15 Ci
	Concrete-TRU Ash	0.0005-0.035	heated, 15 Ci
	Asphalt	0.15-0.76	7.7 Ci
THERMAL	Paper	1.3	70°C
	Polyethylene	1.9	70°C
	Composite	0.02-0.2	40°C, calc.
BACTERIAL	Composite, Test 1	Aerobic//Anaerobic	
		0.9//1.2	25°C
	Composite, Test 2	12//32	50°C
		0-1.6//0.3-4.2	25°C
	Plywod Box	1.3-5.5//0.6-7.8	40°, 70°C
		0-14//11-26	25°C
Asphalt	2.8-19//6.8-23	40°, 70°C	
	0.1-2.6//0-4.8	25°C	
		0-8.4//0-1.9	40°, 70°C
CORROSION	Mild Steel	2.0	wet, deaerated
ALPHA DECAY	He Generation	3.7×10^{-8}	0.039 Ci
		1.5×10^{-5}	15 Ci

July 1979

- (e) The bacterial gas production from plywood, used for FRP plywood boxes, yields potentially the largest source of gas; this is due to the bacterially nutritious cellulosic content of the plywood and its large relative mass.

The magnitude, potential, and uncertainty in bacterial gas generation rates from organic matrices require further study in the areas mentioned above for adequate resolution. This experimental effort is continuing.

Thermal

A large uncertainty exists in the measured thermal gas production at 70° and 100°C, and in the calculated rate at 40°C. This uncertainty results from slow generation rates since there are no experimental means for acceleration--other than raising the temperature.

- (a) No data are yet available on gas generation as a function of time at 40°C; it is assumed that the rate will decrease with time (but how fast is unknown).
- (b) Salt (NaCl) appears qualitatively to catalyze the degradation of polyethylene and paper at 40°C; FeCl₂, another potential in-mine catalyst, appears to do likewise for paper (cellulosics).
- (c) It is assumed that thermal degradation at 25°C will be negligible.
- (d) Water vapor release, the thermal dewatering of process sludges, can be quite significant, even at 25°C.

Radiolysis

This is the area of TRU waste degradation that has been most thoroughly characterized.

- a. A dose rate effect on gas production has been tentatively identified. For some existing data, an initial gas production rate can be calculated (shown in Table 13). For high dose rates, gas production will decrease exponentially as a function of time, primarily due to localized matrix depletion near individual alpha-emitting particles. For existing TRU-contaminated wastes with an average very low dose rate/plutonium loading, the gas production rate may remain fairly constant for hundreds of years.
- b. A pressure effect on gas generation rates, for cellulosics and plastics, was observed at pressures as low as 0.7 MPa (100 psi). Increasing pressure resulted in decreased gas production. At a pressure of 10 MPa (1500 psi), radiolytic gas generation essentially ceased. This pressure effect could have a significant impact on total quantities of gas that can be generated before assumed back-reactions become effective. No pressure effect has been noted for concrete waste systems up to 1.4 MPa (200 psi).
- c. Temperature was found to have a synergistic effect on radiolytic gas generation. A 43 percent increase in gas generation rate was

noted for a temperature increase of 30°C (from 20°C to 50°C) and a 50°C increase (from 20°C to 70°C) produced a 70 percent increase. This effect decreases in importance with time. At 70°C, this increase in rate has, after several months, apparently leveled off at +30 percent.

- d. Explosive concentrations of radiolytically generated gases have been found at LASL (3) in trench-stored, highly ²³⁸Pu-contaminated (remote handled) drums of organic matrix wastes. This will require caution in handling such wastes. Routine gas sampling and analysis, venting, or replacement of in-drum gases with an inert gas, for such wastes has been suggested.

Corrosion

Hydrogen gas will be generated by a corrosion mechanism only in an anaerobic (anoxic) and inundated or wet storage environment. In an air atmosphere, with moisture present, oxygen gas will be consumed. The corrosion rates measured for mild steel can be applied, as upper limits, to TRU-contaminated metal scrap as well as the 210-liter waste drum. Under expected repository environmental conditions, the corrosion of steel is not expected to yield significant quantities of gas.

In order to put gas generation into perspective by individual mechanism, the total amounts of gas generated per year, per unit (Table 2) drum of existing and developmental TRU waste matrices are listed in Table 14 and illustrated in Figure 7. Values specified are most probable gas generation ranges (in parentheses), based on measured data, plus approximate upper and lower limits, taking into account estimated uncertainties in the measured data.

The last rate column shown in Figure 7 is the calculated "overall average" gas generation rate per drum, based on the existing inventory of defense TRU wastes temporarily stored at the Idaho National Engineering Laboratory (13), excluding process sludges. The overall rate is averaged on a waste volume basis and is heavily weighted by the bacterial degradation of organic matrix wastes. The lower overall average rate limit is based primarily on the radiolysis rate of organic composite wastes; the upper rate limit is based on the most probable bacterial rate range but, conservatively, with an additional 100 percent uncertainty included.

The dashed-line upper uncertainties for plywood-box bacterial-degradation rates shown in Figure 7 represent data for an entire 4 x 4 x 7 foot (3.2 m³) FRP plywood box. The corresponding most probable ranges and uncertainty limits (solid lines) for an FRP plywood box having the same volume as a 210-liter drum are also indicated on Figure 7 and in Table 14. The ratio of various plywood box surface areas was utilized for calculating such values.

Based on the experimental data presented, we can rank order the relative quantities of gas generated by individual mechanism for existing forms of

TABLE 14

COMPARATIVE GAS GENERATION RATES

<u>Mechanism</u>	<u>Matrix</u>	<u>Gas Limits</u> (moles/year/drum)*
BACTERIAL	Composite, Aerobic	0-(0.9-5.5)-12**
	Composite, Anaerobic	0-(1.2-4.2)-32
	Plywood Box,* Aerobic	0-(0.44-2.2)-3.0
	Plywood Box,* Anaerobic	0-(1.1-3.7)-4.1
	(Plywood Box, Aerobic, 3.2 m ³)	0-(2.8-14)-19
	(Plywood Box, Anaerobic, 3.2 m ³)	0-(6.8-23)-26
	Asphalt, Aerobic	0-(0.1-2.6)-8.4
	Asphalt, Anaerobic	0-(0-1.9)-4.8
THERMAL	Composite (40°C)	0-(0.02-0.2)-0.4
	Paper (70°C)	0.5-(1.3)-2
RADIOLYSIS	Cellulosics	0.002-(0.005-0.011)-0.012
	Polyethylene	0.003-(0.007)-0.008
	PVC	0.01-(0.03-0.042)-0.08
	Composite	0.002-(0.005)-0.006
	Asphalt (7.7 Ci)	0.1-(0.15-0.76)-1.0
	Concrete-TRU Ash (poured, 15 Ci)	0.03-(0.045-0.93)-1.0
	Concrete-TRU Ash (heated, 15 Ci)	0.0002-(0.0005-0.035)-0.05
CORROSION	Mild Steel	0-(0)-2.0
ALPHA DECAY	He Generation	0.00002
OVERALL AVERAGE (Volume Basis)	Existing INEL TRU Wastes	0.0005-(0.3-1.4)-2.8 per drum
	or	0.003-(1.5-6.8)-13.5 per m ³
	or	0.0001-(0.042-0.19)-0.38 per ft ³

*drum volume = 0.21 m³

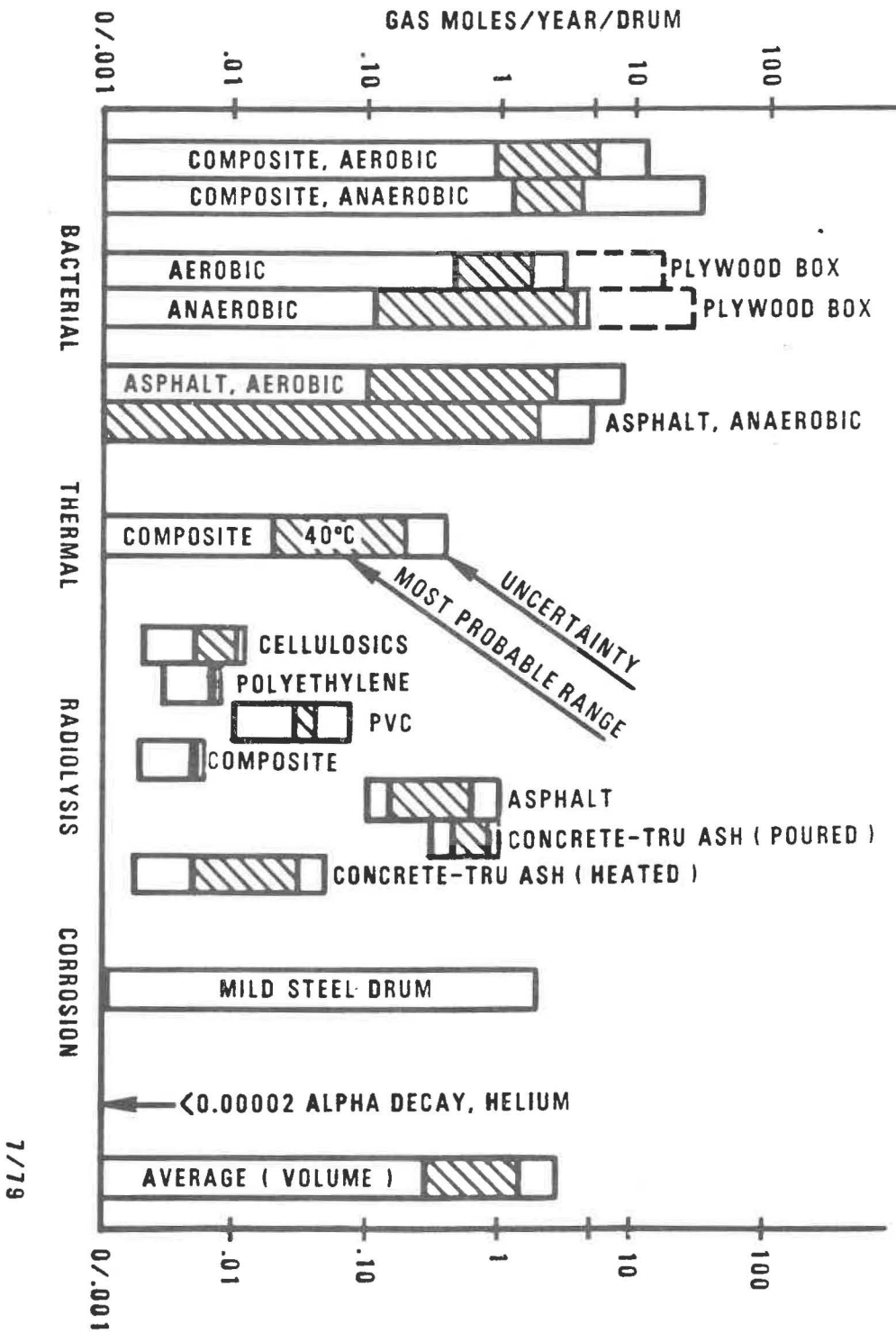
**lower limit-(most probable range)-upper limits; with estimated uncertainties.

July 1979

COMPARATIVE GAS GENERATION RATES
MOLES/YEAR/DRUM

 Sandia Laboratories

FIGURE 7



TRU-contaminated wastes under expected WIPP environmental conditions:

1. BACTERIAL (greatest potential, but large variability)
2. THERMAL (at 40°C; probably insignificant at 25°C)
3. RADIOLYSIS (potential short-term risks)
4. CORROSION (dry conditions)

For comparative purposes, the calculated theoretical maximum number of gas moles generated--if all waste from materials and container were degraded into gaseous species by a combination of probably incredible mechanisms (under reference repository conditions) in an aerobic (air) atmosphere--is listed in Table 15. This total calculated number of moles of gaseous products, 5600, could probably never be achieved in a real-world situation other than by high temperature incineration. Bacterial, thermal, and radiolytic degradation of the organic composite waste matrix listed would probably yield a significant fraction of solid degradation by-products. Such solid by-products would be subject to further degradation, under WIPP-specific environmental conditions, only with great difficulty and at extremely slow (comparative) rates. Also, the plastic component of the composite waste is relatively immune to bacterial degradation. It is estimated that the maximum number of moles of gas species to be generated from a drum of organic composite, TRU contaminated waste will be approximately 2000 moles total.

The processing of existing forms of organic, combustible wastes (e.g., by incineration, slagging, digesting, etc.), followed by ash encapsulation in a suitable immobilization matrix (e.g., glass, heated concrete, slag, etc.) could greatly reduce or eliminate gas generation by bacterial, thermal, and (most) radiolytic degradation mechanisms. TRU ash encapsulation in a heated (or nitrite-containing) concrete matrix appears quite promising. Probable benefits gained by waste processing include volume reduction and ease of transportation (volume, package design, accident scenarios leading to dispersion, etc.). Processing of non-organic, non-combustible TRU-contaminated wastes such as metal scrap, discarded glassware, decontaminated facility rubble, e.g., the majority of TRU wastes, would yield very little reduction of total gas generation. Compared to organic matrix waste, the non-combustible materials generate very little gas.

Assessing the impact of gas generation from organic combustible wastes requires consideration of other factors. The gas generation data presented are the input for long-term gas accumulation/pressurization calculations, permeability measurements and analyses, and consequence assessments of mine response to gas generation; these are discussed in detail elsewhere (11).

Short-term considerations on the degradation of organic matrix TRU wastes must also be put into perspective. Radiolysis can and does produce combustible and explosible gas mixtures in drums of trench-stored, highly ²³⁸Pu-contaminated TRU wastes. Radiolysis can also produce quantities of finely divided, relatively highly contaminated and dispersable particulates from the localized depletion of organic materials. These potentially hazardous conditions must be considered for handling, transportation, mine emplacement operations, and for accident scenario consequence assessments related to these operations. The combination of all these analyses is a major consideration in determining whether existing forms of defense-related TRU wastes are acceptable for safe isolation in the WIPP, or whether they must be processed to alternate, more degradation-resistant forms.

TABLE 15

THEORETICAL TOTAL GAS GENERATION/DRUM

(in air atmosphere)

	<u>Weight</u>	<u>Moles/Drum</u>
Steel Drum, 210 liter	25 kg	0
Drum Liner, Polyethylene (C ₂ H ₄) _n	8.6 kg	610 H ₂ 610 CO _x
Organic Composite Waste:	51.4 kg	-
Cellulosics (35 percent) (C ₆ H ₁₀ O ₅) _n	18.0 kg	560 H ₂ 670 CO _x
Polyethylene (23 percent) (C ₂ H ₄) _n	11.8 kg	840 H ₂ 840 CO _x
Polyvinyl (Chloride (12 percent) (C ₂ H ₃ Cl) _n	6.2 kg	150 H ₂ 200 CO _x 50 Cl ₂
Neoprene (15 percent) (C ₄ H ₅ Cl) _n	7.7 kg	220 H ₂ 350 CO _x 60 Cl ₂
Hypalon (15 percent) -(C ₇ H ₁₃ Cl) ₁₂ -(CHSO ₂ Cl) ₁₇ -	7.7 kg	190 H ₂ 220 CO _x 30 Cl ₂ 40 SO _x

Total Gas Moles = 5600 (in air)

7.0 REFERENCES

1. M. A. Molecke, Waste Isolation Pilot Plant Transuranic Wastes Experimental Characterization Program: Executive Summary, SAND78-1356, November, 1978.
2. S. Kosiewicz, B. Barraclough and A. Zerwekh, Los Alamos Scientific Laboratory, Studies of Transuranic Waste Storage Under Conditions Expected in the Waste Isolation Pilot Plant (WIPP), October 1 - December 15, 1978, LA-7649-PR, March, 1979.
3. A. Zerwekh, Gas Generation From Radiolytic Attack of TRU-Contaminated Hydrogenous Waste, LA-7674-MS, June, 1979.
4. N. E. Bibler, Radiolytic Gas Production During Long-Term Storage of Nuclear Wastes, DP-MS-76-51, paper presented at the 28th Southeastern Regional Meeting of the American Chemical Society, Gatlinburg, TN, October, 1976.
5. N. E. Bibler, Gas Production from Radiolysis of Concrete Containing TRU Incinerator Ash, Progress Report for August-November, 1978, DPST-78-150-2, April, 1979.
6. A. Kazanjian, Radiolytic Gas Generation in Plutonium Contaminated Waste Materials, RFP-2469, October, 1976.
7. M. A. Molecke, Gas Generation From Transuranic Waste Degradation: An Interim Assessment, SAND79-0117, October, 1979.
8. B. J. Barnhart, D. E. Caldwell, et al., Potential Microbial Impact on Transuranic Wastes Under Conditions Expected in the Waste Isolation Pilot Plant, October 1 - December 1, 1978, LA-7788-PR, May, 1979.
9. B. J. Barnhart, D. E. Caldwell, et al., Potential Microbial Impact on Transuranic Wastes Under Conditions Expected in the Waste Isolation Pilot Plant, March 15 - June 15, 1979, LA-7918-PR, July, 1979.
10. An Interim Summary of Experimental Programs for the WIPP TRU Waste Acceptance Criteria, Sandia Laboratories, January, 1979, draft.
11. Summary of Research and Development Activities in Support of Waste Acceptance Criteria for WIPP, Sandia Laboratories, SAND79-1305, November 1979.
12. D. E. Maxwell, K. K. Wahi, B. Dial, Science Applications, Inc., The Thermomechanical Response of WIPP Repositories, SAND79-(SAI-FR-145, 10/78).
13. H. C. Shefelbine, Preliminary Evaluation of the Characteristics of Defense Transuranic Wastes, SAND78-1850, November, 1978.

14. S. Kosiewicz, B. Barraclough, and A. Zerwekh, Studies of Transuranic Waste Storage Under Conditions Expected in the Waste Isolation Pilot Plant (WIPP), An Interim Summary Report, October 1, 1977 - June 15, 1979, LA-7931-PR, rough draft.
15. N. E. Bibler, Gas Production from Alpha Radiolysis of concrete Containing TRU Incinerator Ash, Progress Report for April to July, 1978, DPST-78-150-1, February, 1979.
16. N. E. Bibler, Radiolytic Gas Generation in Concrete Made With Incinerator Ash Containing Transuranic Nuclides, DP-MS-079-25, draft, September, 1979.
17. S. Kosiewicz, A. Zerwekh, and B. Barraclough, Los Alamos Scientific Laboratory, Experimental Studies of the degradation of RAD-Wastes for the Sandia Laboratories Waste Isolation Pilot Plant (WIPP), October 1 - December 1, 1977, LA-7246-PR, May, 1978.
18. A. Kazanjian and d. Horrell, Thermal and Radiation Stability of Polyvinyl Chloride, Dow Chemical, USA, RFP-1924, September, 1972.
19. T. N. Bowmer and J. H. O'Donnell, Nature of the Side Branches in Low-Density Polyethylene: Volatile Products from Gamma Radiolysis, Polymer, 18, 1032-40, 1977.
20. D. T. Turner, Polyethylene Terephthalate, in The Radiation Chemistry of Macromolecules, II, Malcom Dole, ed., Academic Press, New York, 137-166, 1973.
21. N. E. Bibler, Curium-244 Alpha Radiolysis of Nitric Acid. Production from Direct Radiolysis of Nitrate Ions, J. Phys. Chem., 78, 211, 1974.
22. G. R. Waterbury and A. Zerwekh, Office Memorandum, TRU Waste Research and development Program A-412, Annual Report for Period January 1 - December 31, 1976, not published.
23. G. R. Waterbury and A. Zerwekh, Office Memorandum, TRU Waste Research and development Program A-412, Annual Report for Period January 1 - December 31, 1977, not published.
24. J. E. Hoy, Savannah River Laboratory, DPST-78-245, February, 1978.
25. K. Grossaint and d. I. Hunter, Rocky Flats Plant, MSL 76-157, unpublished data.
26. D. I. Hunter, Rocky Flats Plant, MSL 76-291, unpublished data.
27. M. E. McLain, Visit to SRL/SRP, Los Alamos Scientific Laboratory trip report H-8-WM-156, April 2, 1974 (unpublished).
28. N. E. Bibler, Radiolytic Gas Production from Concrete Containing Savannah River Plant Waste, DP-1464, January, 1978.

29. I. G. Draganic and Z. D. Draganic, *The Radiation Chemistry of Water*, Academic Press, New York, p. 76, 1971.
30. F. R. McMillan, *Concrete Primer*, American Concrete Institute, p. 16, Detroit, Michigan, 1958.
31. J. A. Stone, *Evaluation of Concrete as a Matrix for Solidification of Savannah River Plant Waste* (p. 70), DP-1448, 1977.
32. Memorandum, N. Bibler, to J. Kelley, Savannah River Laboratory, Report of Visit by Mound Laboratory Waste Immobilization Personnel, DPST-79-254, February 8, 1979 (unpublished).
33. J. G. Moore, E. Newman, G. Rodgers, *Radioactive Waste Fixation in FUETAP (Formed Under Elevated Temperature and Pressure) Concretes - Experimental Program and Initial Results*, ORNL/TM-6573, March, 1979.
34. S. Kosiewicz, B. Barraclough, and A. Zerwekh, *Studies of Transuranic Waste Degradation Under Conditions Expected in the Waste Isolation Pilot Plant (WIPP)*, December 15, 1978 - March 15, 1979, LA-7775-PR, May, 1979.
35. R. Salovey, "PolyVinyl Chloride," in *Radiation Chemistry of Macromolecules, II*, Malcolm Dole, ed., Academic Press, NY, p. 37-45, 1973.
36. *Proceedings on Bituminization of Low and Medium Level Radioactive Wastes*. Seminar organized jointly by the OECD Nuclear Energy Agency and the Eurochemic Company, Antwerp, Belgium, May 18-19, 1976, ISBN 92-64-01509-4.
37. G. Pretschner and A. Dagen, "Untersuchung zum Wasserstoff und Methanbildung bei der Bestrahlung von Bitumen B-45 und Gemischen aus Bitumen B-45 und Feststoffen," CONF-761260, SAAS-220, p 28-38, December, 1976.
38. J. A. Stone, *Separation of SRP Waste Sludge and Supernate*, DP-1441, 1976.
39. J. A. Kelley, *Evaluation of Glass as a Matrix for Solidification of Savannah River Plant Waste: Nonradioactive and Tracer Studies*, 1975.
40. J. A. Kelley, *Evaluation of Glass as a Matrix for Solidification of Savannah River Plant Waste Radioactive Studies*, DP-1397, 1975.
41. J. A. Kelley and N. E. Bibler, *Effects of Internal Alpha Radiation on Borosilicate Glass Containing Savannah River Plant Waste*, DP-1482, May, 1978.
42. A. Zerwekh, S. Kosiewicz, *Experimental Studies of the Degradation of RAD-Wastes for the Sandia Laboratories Waste Isolation Pilot Plant (WIPP)*, January 1 - March 31, 1978, LA-7259-PR, June, 1978.

43. A. Zerwekh, S. Kosiewicz, Experimental Studies of the Degradation of RAD-Wastes for the Sandia Laboratories Waste Isolation Pilot Plant (WIPP), April 1 - June 30, 1978, LA-7478-PR, October, 1978.
44. S. Kosiewicz, B. Barraclough, A. Zerwekh, and B. Barnhart, Studies of Transuranic Waste Storage Under Conditions Expected in the Waste Isolation Pilot Plant (WIPP), July 1- September 30, 1978, LA-7582-PR, January, 1979.
45. Mudge, et. al., Battelle Pacific Northwest Laboratory, Waste Treatment and Handling Processes Annual Report, BNWL-1861, September, 1974.
46. H. W. Godbee, Spontaneous Combustion, Oxidation and Pyrolysis of combustible Solid Transuranic Contaminated Wastes in Combustible and Non-Combustible Containers, ORNL-4768, May, 1972.
47. A. Zerwekh, Los Alamos Scientific Laboratory, unpublished data, 1973 and 1977.
48. E. J. Murphy, J. Polymer Science, 58, 649, 1962.
49. C. E. ZoBell and M. A. Molecke, Survey of Microbial Degradation of Asphalts with Notes on Relationship to Nuclear Waste Management, SAND78-1371, December, 1978.
50. D. E. Caldwell, University of New Mexico, Microbial Biogeochemistry of WIPP Wastes, Quarterly Report, June 1-30, 1978, unpublished.
51. B. J. Barnhart, D. E. Caldwell, et al., Potential Microbial Impact on Transuranic Wastes Under Conditions expected in the Waste Isolation Pilot Plant, December 15, 1978 - March 15, 1979, LA-7839-PR, July, 1979.
52. B. J. Barnhart, D. E. Caldwell, et al., Potential Microbial Impact on Transuranic Wastes Under Conditions expected in the Waste Isolation Pilot Plant, March 15, 1979 - June 15, 1979, LA-7918-PR, July, 1979.
53. J. A. Cole, Microbial Gas Metabolism, Adv. Microbial Physiology, 14, 1-92, 1977.
54. Werner and Pfeleiderer Corporation, Radwaste Solidification Process for Low-Level Waste and Radioactive Residues, their Origin and Elimination, 1977, unpublished brochure.
55. P. J. Weimer and J. G. Zeikus, Fermentation of Cellulose and Cellobiose by Clostridium Thermocellum in the Absence and Presence of Methanobacterium Thermoautotrophicum, Applied Environmental Microbiology, 33, 289-297, 1977.
56. A. W. Khan, Anaerobic Degradation of Cellulose by Mixed Culture, Canadian Journal of Microbiology, 23, 1700-1705, 1977.

57. A. W. Khan and T. M. Trotter, Effect of Sulfur-Containing Compounds on Anaerobic Degradation of Cellulose to Methane by Mixed Cultures Obtained from Sewage Sludge, Applied Environmental Microbiology, 35, 1027-1034, 1978.
58. D. L. Crawford, Lignocellulose Decomposition by Selected Streptomyces Strains, Applied Environmental Microbiology, 35, 1041-1045, 1978.
59. P. D. O'Brien, Sandia Laboratories, personal communication, June, 1979.
60. J. W. Braithwaite and W. L. Larson to M. A. Molecke, Sandia Laboratories, memo, Status report of TRU Waste Container Compatability Program, August 18, 1978, unpublished.
61. J. W. Braithwaite to M. A. Molecke, Sandia Laboratories, memo, Status Report on Corrosion Yielding Gas Generation, June 14, 1979, unpublished.

DISTRIBUTION:

U.S. Department of Energy, Headquarters
Office of Nuclear Waste Management
Washington, DC 20545

Eugene F. Beckett, Project Coordinator (WIPP) (1)
Colin A. Heath, Director, Division of Waste Isolation (2)
Sheldon Meyers
Raymond G. Romatowski
R. Stein
Carl L. Cooley

U.S. Department of Energy, Albuquerque Operations
P.O. Box 5400
Albuquerque, NM 87185

D. T. Schueler, Manager, WIPP Project Office (2)
R. Rudolph, Acting Deputy Manager, WIPP Project Office
G. Dennis, Director, Public Affairs Division
S. C. Taylor, C&TI Division (for Public Reading Rooms)

U.S. Department of Energy
Carlsbad WIPP Project Office
Room 113, Federal Building
Carlsbad, NM 88220

U.S. Department of Energy
c/o Battelle
Office of Nuclear Waste Isolation
505 King Avenue
Columbus, OH 43201

Jeff O. Neff

Battelle Memorial Institute
Office of Nuclear Waste Isolation
505 King Avenue
Columbus, OH 43201

Neil Carter, General Manager (3)
R. Heineman
Wayne Carbiner
R. Robinson
S. Matthews
A. A. Bauer
J. F. Kircher
D. Moak
F. O'Hara
W. Hewitt

Westinghouse Electric Corporation
P.O. Box 40039
Albuquerque, NM 87196

R. C. Mairson
D. Hulbert
V. F. Likar
H. H. Irby
A. K. Kuhn, D'Appolonia

Hobbs Public Library
509 N. Ship St.
Hobbs, NM 88248
Ms. Marcia Lewis, Librarian

Lokesh Chaturvedi
Department of Civil Engineering
Box 3E
New Mexico State University
Las Cruces, NM 88003

National Academy of Sciences, WIPP Panel

Frank L. Parker, Chairman
Department of Environmental and
Water Resources Engineering
Vanderbilt University
Nashville, TN 37235

Konrad B. Krauskopf, Vice Chairman
Department of Geology
Stanford University
Stanford, CA 94305

Neville G. W. Cook, Member
Dept. of Material Sciences and Engineering
University of California at Berkeley
Heart Mining Building, #320
Berkeley, CA 94720

Merril Eisenbud, Member
Inst. of Environmental Medicine
New York University Medical Center
Box 817
Tuxedo, NY 10987

Fred M. Ernsberger, Member
Glass Research Center
PPG Industries, Inc.
Box 11472
Pittsburgh, PA 15238

Roger Kasperson, Member
Center for Technology, Environment and Development
Clark University
Worcester, MA 01610

Richard R. Parizek, Member
Department of Hydrogeology
Pennsylvania State University
University Park, PA 16802

National Academy of Sciences, WIPP Panel

Thomas H. Pigford, Member
Department of Nuclear Engineering
University of California
Berkeley, CA 94720

Roger W. Staehle, Member
Dean, Institute of Technology
University of Minnesota
Lind Hall
Minneapolis, MN 55455

John W. Winchester, Member
Department of Oceanography
Florida State University
Tallahassee, FL 32306

D'Arcy A. Shock, Consultant
233 Virginia
Ponca City, OK 74601

John T. Holloway, Executive Secretary
2101 Constitution Avenue, NW
Washington, DC 20418

WIPP Public Reading Room
Atomic Museum, Kirtland East AFB
Albuquerque, NM 87185
Attn: Ms. Gwynn Schreiner

WIPP Public Reading Room
Carlsbad Municipal Library
101 S. Hallagueno St.
Carlsbad, NM 88220
Attn: Lee Hubbard, Head Librarian

Thomas Brannigan Library
106 W. Hadley St.
Las Cruces, NM 88001
Attn: Don Dresp, Head Librarian

Roswell Public Library
301 N. Pennsylvania Avenue
Roswell, NM 88201
Attn: Ms. Nancy Langston

Dr. Bruno Giletti, Co-Chairman
Department of Geological Sciences
Brown University
Providence, Rhode Island 02912

Dr. Raymond Siever, Co-Chairman
Department of Geological Sciences
Harvard University
Cambridge, Massachusetts 02138

Dr. John Handin, Director
Center of Tectonophysics
Texas A & M University
College Station, Texas 77840

Dr. John Lyons
Department of Earth Sciences
Dartmouth College
Hanover, New Hampshire 03755

Dr. George Pinder
Department of Civil Engineering
Princeton University
Princeton, New Jersey 08540

New Mexico Advisory Committee on WIPP
NMIMT Graduate Office
Socorro, NM 87801
Marvin H. Wilkening, Chairman (2)

State of New Mexico
Environmental Evaluation Group
320 Marcy Street
P.O. Box 968
Santa Fe, NM 87503
Robert H. Neill, Director (2)

NM Department of Energy & Minerals
P. O. Box 2770
Santa Fe, NM 87501
Larry Kehoe, Secretary
Kasey LaPlante, Librarian

Bechtel Inc.
P. O. Box 3965
San Francisco, CA 94119
R. A. Langley
H. G. Taylor
P. K. Frobenius
D. L. Roberts
D. Duncan
J. Birkmyer

J. E. Magruder
Sandia Carlsbad Representative
401 North Canal Street
Carlsbad, NM 88220

Paul W. Levy
Physics Department
Brookhaven National Laboratory
Associated Universities, Inc.
Upton, Long Island, New York 11973

U. S. Department of Energy
Idaho Operations Office
Nuclear Fuel Cycle Division
550 Second Street
Idaho Falls, ID 83401

R. M. Nelson
J. Whitsett

R. E. Gerton
U. S. Department of Energy
Richland Operations Office
Nuclear Fuel Cycle & Production Division
P. O. Box 500
Richland, WA 99352

U. S. Department of Energy
Savannah River Operations Office
Waste Management Project Office
P. O. Box A
Aiken, SC 29801

J. R. Covell
D. Fulmer

D. E. Large
U. S. Department of Energy
Research & Technical Support Division
P. O. Box E
Oak Ridge, TN 37830

Rockwell International
Rocky Flats Plant
Golden, CO 80401

W. S. Bennett
C. E. Wickland
L. Smith
M. Greinitz

Los Alamos Scientific Laboratory
Los Alamos, NM 87545
Attn: B. J. Barnhart, H-9 (1)

T. K. Keenan, H-7
D. F. Petersen, H-DO
G. R. Waterbury, CMB-1
A. Zerwekh, CMB-1
S. Kosiewicz, CMB-1

Oak Ridge National Laboratory
Box Y
Oak Ridge, TN 37830
Attn: R. E. Blanko

L. R. Dole
K. Haff
J. G. Moore

E. I. Dupont de Nemours Company
Savannah River Laboratory
Aiken, SC 29801

E. L. Albenisius
N. E. Bibler
J. R. Wiley

Argonne National Laboratory
9700 South Cass Avenue
Argonne, IL 60439

S. Fried
A. M. Friedman
L. Jardine
M. Steindler

Mound Research Corporation
Mound Laboratory
Miamisburg, OH 45342

J. W. Doty
K. V. Gilbert

Brookhaven National Laboratory
Department of Applied Sciences
Upton, NY 11973

P. Colombo
R. M. Nielson

University of New Mexico
Biology Department
Albuquerque, NM 87131

D. E. Caldwell

Battelle Pacific Northwest Laboratories
Battelle Boulevard
Richland, WA 99352

D. J. Bradley
R. J. Serne
C. R. Palmer

C. E. ZoBell, A-002
Scripps Institute of Oceanography
University of California, San Diego
La Jolla, CA 92093

U. S. Department of Energy
Division of Waste Products
Mail Stop B-107
Washington, DC 20545

G. H. Daly
J. E. Dieckhoner

Sandia Internal:

1520 T. L. Pace
3310 W. D. Burnett
3313 A. L. Stanley
3141 T. L. Werner (5)
3151 W. L. Garner, For: DOE/TIC (Unlimited Release) (3)
3154-3 R. P. Campbell, For: DOE/TIC (25)
4500 E. H. Beckner
4510 W. D. Weart
4511 W. D. Weart (Acting)
4511 G. E. Barr
4512 T. O. Hunter (10)
4512 C. L. Christensen
4512 D. R. Fortney
4512 M. A. Molecke (25)
4512 A. R. Sattler
4512 J. R. Wayland
4514 M. L. Merritt
4514 F. W. Bingham
4540 M. L. Kramm
4541 L. W. Scully
4541 P. D. O'Brien
4541 H. C. Shefelbine
4541 W. E. Wowak
4542 Sandia WIPP Central Files (2)
4530 R. W. Lynch
4537 L. D. Tyler
4538 R. C. Lincoln
5812 C. J. Northrup
5812 R. G. Dosch
5812 B. T. Kenna
5812 E. J. Nowak
5831 N. J. Magnani
5831 J. W. Braithwaite
8266 E. A. Aas (2)